

Analysis and Experiments
in Preparation for Quantum State Storage
in a Gas of Rubidium Atoms

Master's thesis
by
Karin Hellqvist

Lund Reports on Atomic Physics, LRAP-336
Lund, December 2004

Abstract

Storing quantum information carried by light is a challenge currently addressed within quantum information science. The objective of this master's thesis is to carry out experimental work in preparation for quantum state storage. The scheme, that the experimental work is based on, utilizes photon echoes and the inhomogeneous broadening in a gas of atoms. The experiments consist of carrying out photon echoes in a gas of Rubidium atoms. The theory of photon echoes and the theory of the specific quantum state storage scheme, which the thesis is built on, are described. Experiments consisting of generating light pulses and detecting photon echoes have been carried out, and the results are given. The equipment used in the experiments is described in some detail. Further experimental work to be carried out, on the way to quantum state storage, is discussed. Calculations on the requirements for realization of quantum state storage in Rubidium are presented.

Contents

Introduction	1
Quantum state storage	2
2.1 Photon echoes	2
2.1.1 Schematic description of a photon echo	2
2.1.2 Description of a photon echo using solutions to Schrödinger's equation	5
2.2 Quantum state storage	6
2.2.1 Requirements for quantum state storage	8
Rubidium	10
3.1 The levels of Rubidium	10
3.2 Optical pumping	12
Equipment	13
4.1 The laser	13
4.2 The electro-optic modulators	13
4.3 The high voltage switches	14
4.4 The acousto-optic modulator	15
4.5 Electrical equipment	17
4.6 Additional optical components	17
4.7 The cell and the heating	17
4.8 The detection	17
Experimental procedure and results	19
5.1 Generating a short pulse	19
5.1.1 Generating a pulse with EOMs	19
5.1.2 Generating a pulse with an AOM	23
5.2 Finding Rubidium absorption peaks	27
5.3 Detecting an echo	28
Further analysis of experiments	33
6.1 Long-lived three-pulse echo	33
6.2 Three-level echo with counterpropagating pulses	34
Conclusions	36
Acknowledgements	37
Bibliography	38
Appendix A	39
Appendix B	43

Chapter 1

Introduction

Photons are an ideal carrier of information since they travel fast and interact less with the surroundings than other information-carrying particles. The problem with photons is however that the information they are carrying is hard to store and recall. Finding a way of storing an arbitrary quantum state of a photon is a step along the way of developing quantum computers. It would also have great importance in the field of quantum cryptography. The storing of the state should be reversible, and the original state should be reconstructed with a high efficiency.

There are several different approaches to solving the problem with storing quantum information carried by light. Yet it is not known which one will be the most useful. Scientific research is done on the different methods, in several research groups around the world. A lot of theories have been presented, but not as much experimental work has been done yet within the field. The different approaches utilize different materials. For example quantum storage schemes has been suggested in single atoms, ensembles of atoms, impurities in solid materials and in quantum dots. A lot of articles can be found on quantum state storage. As an example of a method, one that is based on using single trapped ions and cavity quantum electrodynamics (QED) can be said, [1]. Another method is based on electromagnetically induced transparency (EIT) [2], [3]. The different methods store more, or less, of the different parts of the quantum information carried by photons. An example of such a part can be the information saved in the polarisation of a photon. The methods also have different prospect to achieve long storage times and high reliability.

The approach to quantum state storage behind this master's thesis is built on reversible inhomogeneous broadening, in a gas of atoms. Serguei Moiseev and Stefan Kröll proposed the theory in 2001 [4]. No experimental work has been carried out so far, to see if the theory holds in reality. The aim of this master's thesis was to prepare for the experiment of conducting quantum state storage, according to the suggested scheme. The preparation consisted of achieving high efficiency photon echoes in a gas of Rubidium atoms. The efficiency of the process was to be investigated as well. After this scheme was proposed some similar techniques based on inhomogeneous broadening in solid materials was suggested [5], [6]. These materials will probably be of more use since they are more practical.

In the rapport different aspects of the realisation of quantum state storage are given. In Chapter 2 the theory behind two-pulse photon echoes and the quantum state storage scheme is presented. Besides explaining how the echoes are formed in the two cases, some of the requirements for the quantum state storage are described. In Chapter 3 some optical properties of Rubidium atoms are given, since this is the system used in the experiments. Chapter 4 deals with the experimental equipment. In Chapter 5 the experimental procedure, consisting of generating light pulses and detecting two-level echoes, is explained. The results are given and discussed in this chapter as well. In Chapter 6 some thoughts about further experiments, on the road to realisation of quantum state storage, are presented.

Chapter 2

Quantum state storage

The quantum state storage scheme, which is treated in this chapter, is built on photon echo techniques. Therefore the theory of photon echoes will first be described. An explanation of the quantum state storage scheme is then given.

2.1 Photon echoes

In a photon echo a group of atoms sends out coherent radiation in form of a pulse, some time after they have been excited. In such a case the radiation sent out by the atoms does not follow the ordinary exponential decay, which are normally seen. To prepare for the echo an excitation sequence of two or more successive light pulses is used. The radiation sent out can be regarded as an echo of one or more of the excitation pulses. Two descriptions of the photon echo process will be given in this section. First a schematic description of the interaction between the light and the atoms, in the process, is given [7]. The formation of photon echoes is then described by analysing the solutions of Schrödinger's equation.

2.1.1 Schematic description of a photon echo

The easiest way to explain the formation of an echo is by modelling the atoms as two-level atoms, where electrical dipole transitions between the two levels are allowed. In the two-level model any influences from other levels are neglected. The wave functions for the two levels are given by

$$\psi_k(\vec{r}, t) = \phi_k(\vec{r}) \cdot e^{-i\omega_k t}$$

where k stands for the ground state, g , or the excited state, e . The wave function for an electron in a superposition of these states is

$$\psi(\vec{r}, t) = c_g(t)\psi_g + c_e(t)\psi_e$$

The squares of the coefficients in front of the wave functions, $|c_k|^2$, give the probability of finding the electron in the corresponding state. The coefficients c_k is called the probability amplitudes. If the atom initially is in the ground state, c_e is zero and $\psi = \psi_g$. A photon, or an electromagnetic field in general, interacting with the atom at this stage, can move the wave function all the way up to the excited state so that c_g becomes zero. Or it could just change the coefficients c_k a little. If neither of the c_k is zero the atom is said to be in a superposition of states. The atom will stay in the superposition until it decays to the ground state due to the natural lifetime of the upper state. It can also decay due to other relaxation mechanisms.

An atom in a superposition of states always sends out radiation. The probability of finding the electron in a certain position is given by $|\psi(x, t)|^2$. The probability, and therefore also the atomic charge density, oscillates in time according to

$$\begin{aligned} |\psi(x, t)|^2 &= \psi \cdot \psi^* \\ &= (c_g \phi_g \cdot e^{-i\omega_g t} + c_e \phi_e \cdot e^{-i\omega_e t}) \cdot (c_g \phi_g \cdot e^{-i\omega_g t} + c_e \phi_e \cdot e^{-i\omega_e t})^* \\ &= |c_g|^2 \phi_g^2 + |c_e|^2 \phi_e^2 + c_g c_e^* \phi_g \phi_e \cdot e^{-i(\omega_g - \omega_e)t} + c_g^* c_e \phi_g \phi_e \cdot e^{i(\omega_g - \omega_e)t} \end{aligned}$$

Since the electron is a charge and the oscillation is an accelerated motion, the atom will send out radiation at the transition frequency $\omega_e - \omega_g$.

Consider now a group of atoms, all in the ground state from the beginning. A light pulse, at the transition frequency, comes in and puts the atoms into a superposition state, such that they start oscillating. These oscillations will start in phase with the electrical field of the light pulse. Just after the pulse has passed all the atoms will therefore oscillate in phase. Because of constructive interference, N atoms oscillating in phase will send out a total radiation proportional to N^2 times the intensity from a single atom. This could be compared to N atoms sending out radiation in random phase. These will instead send out a total radiation intensity proportional to just N. If all the atoms in the sample have exactly the same transition frequency, they will continue to oscillate in phase until they have all been deexcited to the ground level.

But consider instead that the atoms have slightly different transition frequencies. Then the atoms will come out of phase with each other shortly after the pulse. The radiation sent out will therefore decrease rapidly. This radiation sent out right after the pulse, before the atoms come out of phase, is called the free induction decay. The differences in frequency, between the atoms, are due to inhomogeneous broadening¹. In a gas the transitions are Doppler broadened. Atoms moving towards the incoming electromagnetic field will experience it as if they had a higher frequency, than the ones moving away from it. The Doppler shift is given by

$$\Delta = \frac{(\omega_e - \omega_g)v}{c}$$

where v is the component of the atom's velocity in the direction of the field. The atoms themselves do not have different transition frequencies, but viewed from the incoming field it appears as if they had. To simplify the explanation, a model where the atoms have different resonance frequencies, $\omega_e - \omega_g + \Delta$, is normally used. The result will be the same, if the atoms are now treated as if they were at rest.

In the first part of Figure 2-1 the population distribution before the first pulse, for a group of atoms, is shown. The inhomogeneous broadening as a function of frequency can be seen. The population distribution after the first pulse is shown in the middle part of the figure. Here the probability of finding the electron in the upper state is the same for all frequency groups of atoms. Now another light pulse is sent in. This pulse should come before too many atoms have decayed to the ground state. On the other hand it should not come too soon, so that it comes in the middle of the free induction decay. The atomic charge density is still oscillating. Because they have slightly different frequency some of the atoms send out radiation in phase with the incoming electrical field, and some send out radiation out of phase. Again looking at interference, it could be seen that the atoms sending out radiation in phase with the field will constructively interfere with the field. The total intensity in this case will increase, which has to be due to stimulated emission. Therefore atoms in phase with the field will be deexcited down to the ground state. Atoms sending out radiation out of phase will on the other hand interfere destructively with the field, resulting in absorption. These atoms will all be moved to the excited state. At this moment there will be a population gratings at the two states. This situation can be seen in the last picture of Figure 2-1.

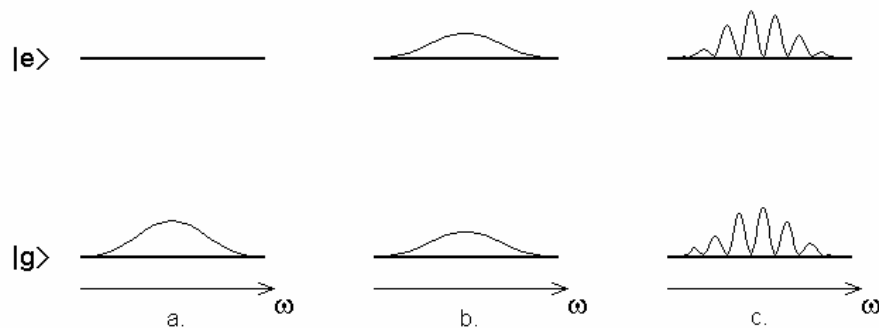


Figure 2-1: The population distribution a. before the first pulse, b. after the first pulse, and c. after half of the second pulse has passed. Atoms in phase

¹ That a broadening mechanism is inhomogeneous means that it is due to that different atoms have different transition frequencies.

The groups of atoms that are no longer in a superposition will not continue to oscillate. As the second pulse continues to irradiate the atoms, the atoms in the upper state will be deexcited since that is the only possibility. The atoms in the lower state will be excited. After the second pulse the atoms will be back in a superposition of both the states. The atoms that were deexcited start oscillating in phase with the field. These were the atoms that were out of phase when the second pulse entered the sample. The other group of atoms, which were in phase before the second pulse, is now out of phase. The second pulse is said to have rephased the atoms. Now as the atoms continue to oscillate, their phase difference will decrease instead of increase, as was the case before the second pulse. The evolution of some atoms can be seen in Figure 2-2. Here only five atoms are shown, but in reality there are many more atoms interfering. At time zero in the figure the first pulse will start the oscillations of all the atoms. The second pulse passes at the time T . The top and bottom ones are in phase with the field of the second pulse, and the middle one is out of phase. These three atoms change their phase by π . The other two atoms in the figure send out radiation that is just between in and out of phase with the field. Therefore the field will not affect these atoms. It can be seen from the figure that at time $2T$ all the atoms will be in phase again. Interfering constructively at this point, the radiation sent out will be again proportional to N^2 times the intensity of a single atom. A light pulse will be emitted. This is the two-pulse photon echo.

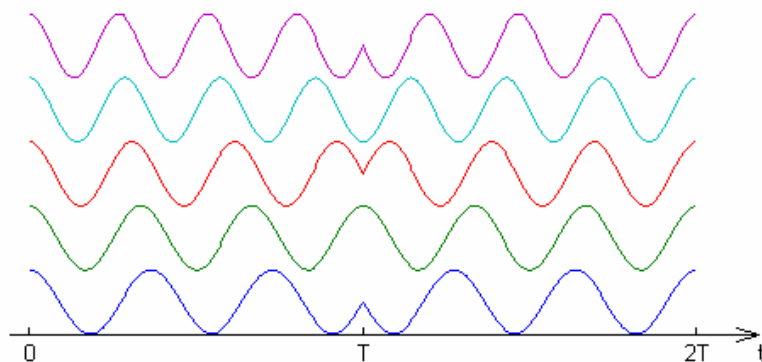


Figure 2-2: Five atoms radiating with slightly different frequencies. From the beginning, after the first pulse, they oscillate in phase. After a time T they are irradiated by a second pulse, and after $2T$ an echo is formed.

In Figure 2-3 the two excitation pulses and the echo are shown. The echo is centred at the time $2T$, as can be seen in the figure. The free induction decay, after the excitation pulses, is also illustrated.

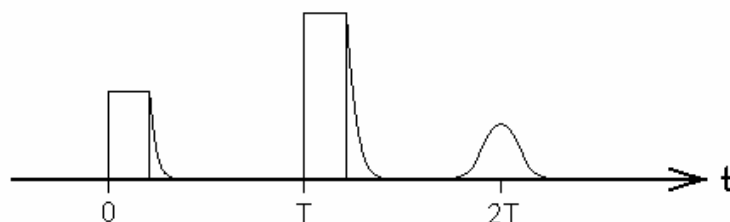


Figure 2-3: Two excitation pulses, with a separation of T , form an echo centred at $2T$. The free induction decay can also be seen after the two excitation pulses.

The intensity of the echo will depend on the intensity of the excitation pulses. The strength of a pulse can be given by the pulse area, θ , defined as

$$\theta = \frac{2\mu E_0 t_p}{\hbar}$$

where μ is the electrical dipole moment for the transition, E_0 is the amplitude of the electromagnetic field, and t_p is the length of the pulse. A light pulse moving all the atoms in a sample all the way from the ground state to the excited state has a pulse area equal to π . It is therefore called a π -pulse. The pulse area can be visualized as an angle of rotation, induced by the pulse. This is done by modelling the two-level atoms as a sphere, where the ground and excited states are the two poles. A vector centred

in the middle of the sphere, and pointing to one of the poles corresponds to all atoms being in that state. If the atoms initially are in the ground state, a rotation of the vector by π will move all the atoms to the excited state. A pulse moving the vector half the way up to the excited state is a $\pi/2$ -pulse. After such a pulse the atoms are in a well-defined superposition of the ground and excited states, where the probabilities of finding the electron in a given state are the same for the two states. The highest echo intensity is achieved if the first pulse is a $\pi/2$ -pulse and the second one is a π -pulse.

The echo will decrease in intensity as the time between the first and second pulse is increased. As more atoms become deexcited, due to the natural lifetime, fewer atoms will contribute to the formation of the echo. Also other homogeneous broadening mechanisms, for example collisions between atoms in gases, will decrease the number of atoms contributing to the echo. This is because these processes will randomise the phase of the atomic wave function. If the optical density of atoms is too low, too much of the excitation pulses will pass the sample without being absorbed. This also leads to a weaker echo since fewer atoms will contribute. If the density is higher the pulses will be absorbed. The problem is then instead that also the echo will be absorbed, and not much of it will leave the ensemble of atoms. Even when an optimum of the atom density is found, the echo intensity is normally only a few percent of the intensity of the first excitation pulse.

2.1.2 Description of a photon echo using solutions to Schrödinger's equation

The formation of a two-pulse photon echo can be derived from Schrödinger's equation, as has been done in Ref. [8]. The solution of the wave function, for an electron, can be presented in the expressions for the probability amplitudes $c_g(t)$ and $c_e(t)$. The probability amplitudes right after a pulse, of pulse area θ , will be²

$$c_g = c_{g0} \cdot \cos(\theta/2) + c_{e0} \cdot i \cdot \sin(\theta/2)$$

$$c_e = c_{e0} \cdot \cos(\theta/2) + c_{g0} \cdot i \cdot \sin(\theta/2)$$

where c_{g0} and c_{e0} are the probability amplitudes right before the pulse. For simplicity the frequency of the ground state has been set to zero, $\omega_g = 0$, and the excited state has a frequency of $\omega = \omega_e - \omega_g + \Delta$. A free evolution in time, of an atom, will give a phase factor of $e^{-i\Delta t}$ in the expression for c_e . This factor give rise to that atoms with slightly different frequency will come out of phase, as described above. Looking at the process of achieving an echo, expressions for the probability amplitudes can be derived at the different time steps. These expressions, for an atom initially in the ground state, are given in Table 2-1. It is assumed that the pulse length is short in comparison with the separation between the pulses. It is also assumed that the coherence time, for the atoms, is long. The homogenous broadening mechanisms are therefore neglected.

	initially	after pulse 1	before pulse 2
$c_e(t)$	0	$i \sin(\theta_1/2)$	$i \sin(\theta_1/2) e^{-i\Delta t}$
$c_g(t)$	1	$\cos(\theta_1/2)$	$\cos(\theta_1/2)$

after pulse 2	some time after pulse 2
$\cos(\theta_2/2) i \sin(\theta_1/2) e^{-i\Delta T} + i \sin(\theta_2/2) \cos(\theta_1/2)$	$[\cos(\theta_2/2) i \sin(\theta_1/2) e^{-i\Delta T} + i \sin(\theta_2/2) \cos(\theta_1/2)] e^{-i\Delta(t-T)}$
$\cos(\theta_2/2) \cos(\theta_1/2) + i \sin(\theta_2/2) i \sin(\theta_1/2) e^{-i\Delta T}$	$\cos(\theta_1/2) \cos(\theta_2/2) + i \sin(\theta_2/2) i \sin(\theta_1/2) e^{-i\Delta T}$

Table 2-1: Coefficients of the wave functions, for the ground and excited state, during the stages in the process of achieving an echo. θ_1 and θ_2 are the pulse areas of the two pulses. t is the time after the first pulse, and T is the time separation between the two excitation pulses.

² A phase factor, due to the position of the electron in space, is not included.

The expressions might look complicated, but they can be simplified by putting in known pulse areas. If the first pulse has a pulse area of $\pi/2$ and the second a pulse area of π , the expressions in Table 2-2 are found.

	initially	after pulse 1	before pulse 2	after pulse 2	some time after pulse 2
$c_e(t)$	0	$i/\sqrt{2}$	$(i/\sqrt{2})e^{-i\Delta t}$	$i/\sqrt{2}$	$(i/\sqrt{2})e^{-i\Delta(t-T)}$
$c_g(t)$	1	$1/\sqrt{2}$	$1/\sqrt{2}$	$-1/\sqrt{2}e^{-i\Delta T}$	$(-1/\sqrt{2})e^{-i\Delta T}$

Table 2-2: Coefficients of the wave functions when the first pulse is a $\pi/2$ -pulse and the second a π -pulse.

It can be seen that after a time $t = 2T$, the two expressions in the last column will have the same phase factor. The atomic dipole moment, for the transition, will then be independent of Δ for all the atoms in the sample. This is because the dipole moment depends on the product $c_g \cdot c_e^*$, which is proportional to $e^{-i\Delta(t-2T)}$. By the dipole moment being independent of Δ , means that all the atoms are oscillating in phase. This is analogous to the result achieved earlier.

2.2 Quantum state storage

The scheme for quantum state storage, presented here, is based on a three-level system, as shown in Figure 2-4. The state denoted $|a\rangle$ is the ground state, $|b\rangle$ the excited state, and $|c\rangle$ the storage state. There are allowed electric dipole transitions between states a and $|b\rangle$, and between $|b\rangle$ and $|c\rangle$. State $|c\rangle$ is a metastable state, meaning that there is no allowed electric dipole transition to $|a\rangle$. State $|c\rangle$ is situated just above state $|a\rangle$.

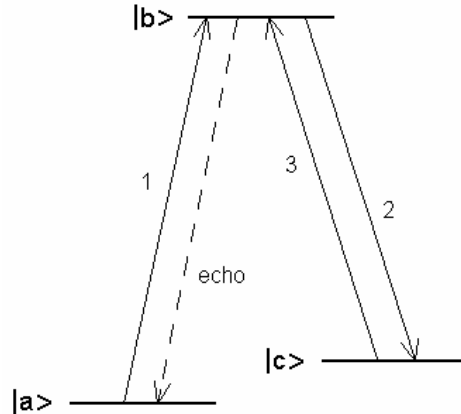


Figure 2-4: The three-level system used for quantum state storage.

The wave function for an atom in the system will be given by

$$\psi(\vec{r}, t) = c_a(t)\psi_a + c_b(t)\psi_b + c_c(t)\psi_c$$

where ψ_a , ψ_b and ψ_c are the wave functions of the three states.

The atoms are all initially in the ground state. Both the excited state and the storage state are empty. A single-photon wave packet, denoted 1 in the figure, puts the atom into a superposition of state $|a\rangle$ and $|b\rangle$. The second pulse is a π -pulse, set to the transition $|b\rangle \rightarrow |c\rangle$. It will move the probability amplitude in the excited state to the storage state. Now the superposition is instead between the ground state and the storage state. Since the storage state is metastable there will be no natural decay of the atoms due to electric dipole transitions. The third pulse is a π -pulse as well. It moves the probability amplitude in the storage state back to the excited state.

If now all the pulses had come from the same direction, the atoms would continue to oscillate more and more out of phase, once they had returned to the excited state. Then there would be no echo. A gas

of atoms however, has the feature that its inhomogeneous broadening is dependent on the direction of the incoming electromagnetic field. The broadening profile for the ensemble of atoms will look the same, but each atom will be positioned at a different place on the profile, for different directions. If the third pulse comes in the direction opposite that of the first photon and the second pulse, the sign of the Doppler shift will be changed for all atoms. The resonance frequencies of an atom will then be $\omega - \Delta$, instead of $\omega + \Delta$. The phase difference between the atoms will in this case start decreasing after the third pulse. At a time after the third pulse, equal to the time between the single photon and the second pulse, an echo of the first photon is generated.

The expressions for the coefficients in the wave function, at different stages in the quantum state storage process, are given in Table 2-3. To shorten the expressions $S_j = \sin(\theta_j/2)$ and $C_j = \cos(\theta_j/2)$ are used, where θ_j is the pulse area of the single photon. T is the time between the single photon and the second pulse, and T_2 is the time between the second and third pulse. Δ_{ab} is the Doppler shift of the transition $|a\rangle \rightarrow |b\rangle$ and Δ_{ac} is the Doppler shift of the frequency difference between state $|a\rangle$ and $|c\rangle$.

	initially	after single photon	before pulse 2	after pulse 2
$c_c(t)$	0	0	0	$-S_j \exp(-i\Delta_{ab}T)$
$c_b(t)$	0	$i S_j$	$i S_j \exp(i\Delta_{ab}t)$	0
$c_a(t)$	1	C_j	C_j	C_j

before pulse 3	after pulse 3	some time after pulse 3
$-S_j \exp(-i\Delta_{ab}T) \exp(-i\Delta_{ac}T_2)$ $\approx -S_j \exp(-i\Delta_{ab}T)$	0	0
0	$-i S_j \exp(-i\Delta_{ab}T)$	$-i S_j \exp(-i\Delta_{ab}T) \cdot \exp(i\Delta_{ab}(t-T-T_2))$
C_j	C_j	C_j

Table 2-3: Coefficients of the wave functions, for the three states, during the stages in the quantum state storage process.

In the expression of c_c before the third pulse the last phase factor has been neglected. It is close to unity because the separation between level $|a\rangle$ and $|c\rangle$ is so small. Therefore the Doppler shift Δ_{ac} is also small. In the last expression of c_b it is apparent that at time $t = 2T + T_2$ the phase factor will disappear. All the atoms are then oscillating in phase, sending out a photon echo. If the content of the table is compared to the content of Table 2-1, some differences can be seen. In the case of the quantum state storage process, the ground state coefficient does not change once the single-photon wave packet has passed. The frequency grating introduced by the first wave packet will not be changed until the echo is released. It can also be seen that now it is the same group of atoms evolving backwards in phase, as was evolving forward before the second pulse. In the two-pulse echo first one group of atoms evolved forward in phase. Then the other group of atoms evolved forward the same amount. Both cases resulting in that all atoms will be in phase again at a certain time.

It has been derived that the echo sent out, in the scheme described above, is the exact time-reversed copy of the single-photon wave packet [4]. In the derivation a lot of approximations and assumptions have been made. These will be discussed later in the next section. The echo is sent out in the opposite direction with respect to the incoming single photon. The pulses and echo direction in the sample of atoms can be seen in Figure 2-5. The density of atoms is high. The dark area shows the probability of absorption of the single photon. The second pulse will interact with the whole volume where the first photon is absorbed. Looking at the time difference between the single photon and the second pulse, it

will be the same for all atoms in the sample, since they both come from the same direction. After the second pulse the superposition is stored until the third pulse comes. The third pulse hits the atoms to the right in the picture first. These atoms will therefore be the ones, which come in phase again first. The echo will travel in the same direction as the third pulse through the sample, being amplified as the atoms along the way will contribute to the echo.

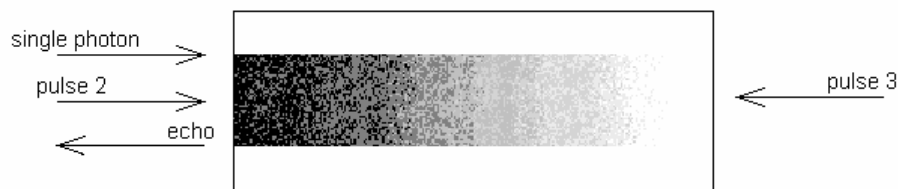


Figure 2-5: Directions of the pulses in and out of the sample of atoms. The dark area shows the probability of absorption of the single photon.

The echo has an efficiency close to unity, of reproducing the quantum state of the single-photon wave packet. The absorption process is replayed in a time-reversed mode, when the echo is formed. The sample of atoms is forced to reemit the exact time-reversed copy, of the single-photon wave packet. It might be hard to realize that the echo, which only consists of a single photon, will not be absorbed on the way out of the sample. This could be understood as follows. The atoms that the echo meets on its way out are still in a superposition of states. It is not until the echo has passed that they will be back in the ground state. The field they are sending out is oscillating in phase with the field of the emitted echo. They will therefore contribute to the echo by stimulated emission, and there will be no absorption. Because of this feature the sample of atoms can be very dense. This was not the case for the two-pulse photon echo described above, were the sample had to have a low density of atoms. In this quantum state reconstruction process, however the sample needs to be dense, to make sure that the single photon is absorbed with a high probability.

2.2.1 Requirements for quantum state storage

For the scheme described in the previous section to work, some requirements must be fulfilled. These are explained in Ref. [9]. The lifetime of the excited state should be greater than the time separation between the single photon and the second pulse. Also the coherence time, of the atoms in the excited state, should be longer than this time separation. The coherence time, of the storage state, should be greater than the storage time. The superposition between the states will be destroyed, with large probability, if either one of these three conditions are not fulfilled.

The spectral width of the second and third pulses should be greater than the spectral width of the single-photon wave packet. Otherwise not all the spectral information in the quantum state of the photon will be stored. The spatial beam size of the two pulses should be much larger than the spatial extent of the photon wave-packet. The atoms, which interacted with the single photon, will otherwise move out of the interaction volume of the second and third pulses before they arrive.

The Doppler broadening, of the transition between the ground and excited state, should be greater than the spectral width of the single-photon wave packet. This is also because the full spectral information of the photon should be stored well. In the wings of the Doppler profile there are fewer atoms absorbing. Therefore the spectral information there will not be stored to the same extent as the information in the centre of the profile.

The transition between the ground and excited state should easily be separated from the transition between the excited and the storage state. One way of doing this is by using a ground state and a storage state that are well separated in energy. The problem then would be that the phase factor neglected in Table 2-3 would play a more important role. The approximation made then would not be as accurate if the separation is large. There is however another way of addressing the transitions one at a time, without interfering with the other. If the levels are different magnetic sublevels, defined by a weak magnetic field, the transitions could be addressed by polarized light. The polarisation of the

different transitions will be different. Therefore it is not a problem if the broadening of the states overlap in energy.

Another important aspect, for the reconstruction of the quantum state to be possible, is that the storage state should initially be empty. If this is not the case, the second and third pulses will interact with the atoms in the storage state. There will be other emitted photons, which might be hard to separate from the echo. With many atoms in the storage state, the second and third pulses would also not be constant throughout the whole sample. They will be approximately constant if there were no atoms in the storage state, except for the stored quantum state. Emptying the storage state by optical pumping could solve this problem, if the ground and storage state are different magnetic sublevels. It is important that the optical pumping is done just before the storage process. Otherwise the pumped atoms will leave the interacting volume, before the pulses enter. Optical pumping will be discussed more in Chapter 3, for the case of Rubidium atoms.

Chapter 3

Rubidium

There are a couple of reasons why Rubidium was chosen as the gas for the quantum state storage experiments. It has a simple system of energy levels. Different magnetic sublevels of the ground state can be used as the initial and storage state. To achieve a high enough atom density, a gas of Rubidium does not have to be heated to more than approximately 80 °C. The lifetime of the excited state is very short, only around 30 ns. This is a disadvantage since the pulses then need to have a very short duration. Ytterbium for example has a lifetime of 875 ns, which would make the experiments much easier. But to achieve the atom density needed, a gas of Ytterbium has to be heated to around 500 °C. For this purpose a special heat-pipe oven would be needed. There are elements that have similar properties as Rubidium that could be used. But since there were lasers available at the right frequency, in the photon echo group, Rubidium was chosen.

3.1 The levels of Rubidium

Rubidium has the atomic number 37 and it belongs to the group of alkali metals in the periodic table. All the elements in this group have one electron in its outermost shell. Rubidium naturally exists in two isotopes. 73 percent in a natural composition of rubidium is ^{85}Rb and 27 percent is ^{87}Rb . In my experiment the ^{87}Rb atoms are used. A lot of information about this isotope and its optical properties can be found in Ref. [10]. The ^{87}Rb isotope has a nuclear spin of 3/2. The electronic transition used in the experiment is between the fine structure levels $5^2\text{S}_{1/2}$ and $5^2\text{P}_{1/2}$, also called the D1 transition. Some data about the D1 transition is given in Table 3-1. The absorption oscillator strength, f , is a dimensionless quantity giving a measure of the transition probability. It is defined as the ratio between the absorption rate of an atom, and the absorption rate of a classical single-electron oscillator [11]. It is given by

$$f_{12} = \frac{2m\omega|\mu|^2}{3\hbar e^2}$$

where μ is the electric dipole moment for the transition.

Frequency	ω_0	$2\pi 377.1074635$ THz
Vacuum wavelength	λ_0	794.9788509 nm
Air wavelength (at 760 torr, 22°C)	λ	794.76569 nm
Lifetime	τ	27.70 ns
Absorption oscillator strength	f_{12}	0.3420

Table 3-1: Some properties of the D1 transition in rubidium.

The hyperfine splitting of the transition can be seen in Figure 3-1. In the experiments the transition used is $F = 2 \rightarrow F' = 2$. The wavelength of this transition is 794.7704 nm in air at a pressure of 760 torr and 22°C.

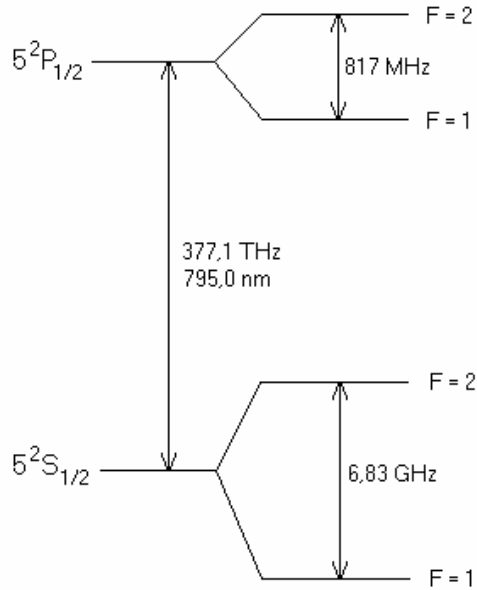


Figure 3-1: The hyperfine splitting of the D1-transition in Rubidium.

In a magnetic field the hyperfine levels will split into levels with different magnetic quantum number. In a weak magnetic field, the splitting is given by the Zeeman effect. The Zeeman splitting for the $F = 2$ state in $^2S_{1/2}$ is 0.70 MHz/G , and for the $F' = 2$ state in $^2P_{1/2}$ it is 0.23 MHz/G^3 . The ground state, in the quantum state storage process, that will be used is the Zeeman level with the lowest quantum number, $m = -2$, in $F = 2$. The excited state will be $m = -1$ in $F' = 2$, and the storage state will be $m = 0$ in $F = 2$. Since electric dipole transitions between different magnetic sublevels are forbidden, the storage state will be metastable. The quantum state storage levels are illustrated in Figure 3-2. The transitions of the pulses in the process can also be seen in the figure. σ^+ -polarised light is used for the single-photon wave packet, where $\Delta m = m_e - m_g = +1$. For the second and third pulse $\Delta m = -1$ and σ^- -polarised light is used. The echo will be σ^+ -polarised.

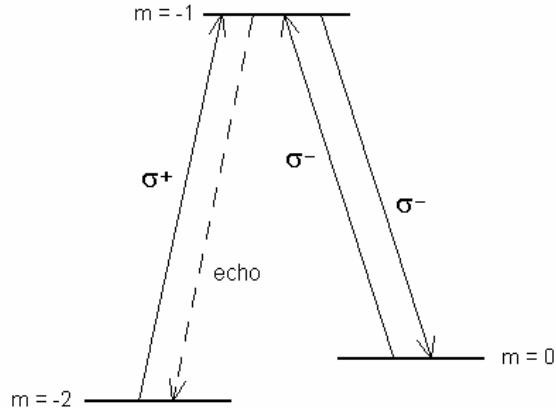


Figure 3-2: The quantum state storage process in the magnetic levels of Rubidium.

The oscillator strength for the transitions between different magnetic levels is given by branching ratios. The branching ratio for the $m = -2, F = 2 \rightarrow m = -1, F' = 2$ transition is $1/6$. This means that the oscillator strength is $0.3420 / 6 = 0.0570$. For $m = 0, F = 2 \rightarrow m = -1, F' = 2$, the branching ratio is $1/4$, leading to $f = 0.0855$. The sum of the oscillator strengths, for all allowed magnetic transitions from one hyperfine level to another, is equal to the total oscillator strength of that transition.

³ Magnetic field strength in gauss: $1 \text{ G} = 10^{-4} \text{ T}$.

3.2 Optical pumping

To prepare all the atoms in the ground state, before the quantum state storage experiment, optical pumping will be carried out. Circularly polarised light, σ^- , will pump $\Delta m = -1$ transitions. A laser set from the hyperfine level $F = 2$ in the $^2S_{1/2}$ state, to $F' = 2$ in the $^2P_{1/2}$ state, will pump this transition. From the excited state the atoms will not only decay to the hyperfine level $F = 2$, but also to the level $F = 1$. Therefore another laser, at wavelength 794.7560 nm, is used to empty the $F = 1$ state. Also this laser is σ^- polarised. The pumping transitions can be seen in figure 3-3.

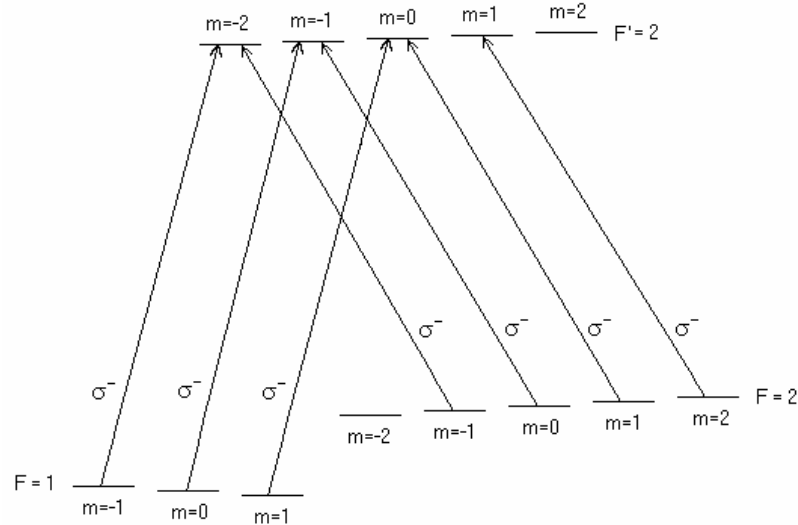


Figure 3-3: Optical pumping using σ^- -polarised light. $m = 2$ in $F = 2$ is the ground state in the quantum state storage scheme. The atoms will be pumped to that state.

Once an atom is excited it will fall down again to one of the hyperfine levels, in the $^2S_{1/2}$ state. Which magnetic level it is deexcited to depend on the probability for the different transitions. Only transitions with $\Delta m = \pm 1$ or $\Delta m = 0$ are allowed electric dipole transitions. Whatever level the atom is deexcited to it will be excited again, except if the atom is deexcited to the $m = -2$ in the ground state. Then it cannot be excited again with the σ^- light, and it will stay in that level. When the pumping has been going on for a while almost all the atoms will be in the $m = -2$ state. This is our ground state, where we want the atoms. Also the storage state $m = 0$ in $F = 2$ will be almost empty, which is even more important.

Calculations of the requirements for quantum state storage in Rubidium can be found in Appendix A. There the intensities of the pulses and the vapour pressure needed are calculated. The Doppler profile for Rubidium atoms is given, and the coherence time is calculated, to see if the requirements for these are fulfilled.

Chapter 4

Equipment

In this chapter the equipment used for the experiments will be described. Most of the items will be introduced briefly. The electro-optic modulator and the acousto-optic modulator will be described in more details. This is because these have played an important part in the experimental work.

4.1 The laser

The experiments were conducted with an external cavity diode laser. The laser has been designed and constructed, as another master's thesis project in the photon echo group [12]. It has a bandwidth of around 300 kHz. The output power varies between 30 and 40 mW, depending on the settings of the current to the diode and the temperature. A Profile LDC 202 diode laser driver is used to deliver current to the diode. The temperature is controlled and stabilised by a Profile TED 200 temperature controller. Coarse tuning of the laser frequency is done by turning the grating, located at one end of the external cavity. Fine adjustment is done by changing the temperature of the diode slightly, or by changing the current through the diode. The laser can be tuned mode-hop free over a range of a few GHz⁴. An electro-optic modulator, inside the external cavity, is used for the tuning. As an electric field is applied over it, its refractive index will be changed and therefore also the length of the cavity. As the electric field is varied the frequency, which depends on the length of the cavity, is changed. A Burleigh pulsed wavemeter, model WA-4500, was used to measure the wavelength of the laser.

The light out from the diode laser has an elliptical cross section. To make the beam more circular an anamorphic prism pair can be used. Depending on how it is turned it can contract in the direction that the beam is extended, making the diameter smaller. Turned the other way it can expand the beam in the direction that it is narrow in, so that the beam becomes larger. This latter way is how the prism pair is used in the experiments. When the beam is larger it will be less divergent.

To avoid reflected light to go back into the laser and disturb it, an optical isolator from Optics For Research, IO-5-793-HP, was used. It consists of a Faraday rotator with a polariser at each end. The rotator will rotate the polarisation 45° independent of the direction the light comes from. The light in the forward direction will be let through by the second polariser. The light in the backward direction however, will be rotated so that the first polariser blocks it.

4.2 The electro-optic modulators

An electro-optic modulator, EOM, is a device that modulates the light in some way. The EOM type used, in the experiments, modulates the polarisation of a light beam. It consists of one or more Pockels cells. A Pockels cell is a crystal, which changes its refractive index when an electric field is applied across it. Perpendicular to the propagation direction, the crystal has two axes with different characteristics. When an electric field is applied across the crystal, light polarised along one of the axis experience one refractive index, and light polarized along the other axis experiences another.

If the light incident on the crystal is polarized at an angle in between the two axes orientations, the light can be regarded as divided into two beams experiencing different refractive indexes. For polarization incident at 45° angle, the light will be divided into two equal parts. As the light travels

⁴ When the laser was built it could be tuned mode-hop free over more than 10 GHz. When the diode inside the laser was changed, to a diode with less efficient anti-reflection coating, the tuning range decreased.

through the crystal, there will be an increasing phase difference between the two beams. The phase difference, after the light has passed the crystal, will depend on the length of the crystal, L , and the difference in refractive index, Δn . It is given by [13]

$$\Delta\varphi = \frac{2\pi}{\lambda_0} L \cdot \Delta n$$

where λ_0 is the wavelength in vacuum. It turns out that the phase difference depends on the applied voltage, U , across the crystal, as follows:

$$\Delta\varphi = \frac{2\pi}{\lambda_0} r \cdot n_0^3 \cdot U$$

where r is the linear electro-optic coefficient, given in m/V. n_0 is the refractive index in absence of an electrical field. If the phase difference after the crystal is π the polarisation will be turned 90° . In this case the Pockels cell functions as a half-wave plate. The voltage, which gives the phase difference π , is called the half-wave voltage, and it is given by:

$$U_{HW} = \frac{\lambda_0}{2r \cdot n_0^3}$$

If the EOM is used together with two polarisers it can modulate the amplitude of the light. One polariser is placed before the modulator, to make the light polarised at an angle of 45° between the two axes of the modulator. Another polariser is placed after the EOM. The two polarisers are rotated so that they are perpendicular to each other. In this way the transmitted light will be extinguished when no field is present across the EOM. This is true when there is no natural birefringence in the crystal. The maximum intensity let through the set-up will occur at the half-wave voltage, when the polarisation is turned 90° . The transmitted intensity, as a function of the applied voltage, U , is given by

$$I = I_{\max} \sin^2\left(\frac{\pi}{2} \frac{U}{U_{HW}}\right)$$

The suppression of the light, through an EOM that is turned off, is often specified as an extinction ratio. It gives a measure of how much light that leaks through when the voltage is turned off, compared to the maximum light through when it is turned on. To get a good extinction ratio it is important that the light goes straight through the modulator crystal, so that no reflections occur inside. Reflections of the beam will destroy the polarisation.

The electro-optic modulators used in the experiments were two Gsänger, LM 0202. They have a half-wave voltage of 200 V at a wavelength of 633 nm. The extinction ratio is given to be 1:250. The capacity between the two plates inside the EOM, which generate the electric field, is 90 pF. To compensate for the crystals natural birefringence, the modulator consists of four crystals. The crystals are placed after each other along the optical axis, rotated from one another by 90° . They are of equal length to minimize the total phase retardation, when no field is present over the modulator. The four crystals are connected electrically parallel, so that the applied field over the nearby crystals are of opposite sign. In this way all the four crystals contribute to the phase retardation induced by the electric field.

4.3 The high voltage switches

To turn on the voltage to the EOMs, two Behlke, HTS 31 and HTS 51, fast high voltage transistor switches were used. These are specified to have a turn-on rise time of less than 5 ns. The turn-off rise time is 50 ns. A high voltage power supply, Model PS350/500V-25W from Stanford Research Systems, provided the high voltage. The trig-signal to the switches was taken from a digital pulse generator, Model DG535, from Stanford Research Systems. The pulse generator gives a square pulse of low voltage, with a fast rise time.

A switch can be coupled in different ways. Two ways that were tested in the experiments are shown in Figure 4-1. The switch can either turn from high to low voltage, or from low to high, when it is triggered. The response from the switch can be changed in different ways. The speed of the switch depends on the resistance in series with the output. The higher the resistance the slower the circuit becomes. A fast circuit is more sensitive to transients in the signal after the switching.

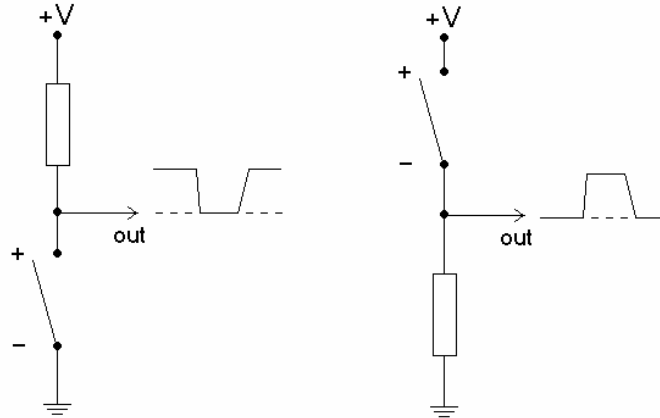


Figure 4-0-1: Different circuit configurations for high voltage switches. To the left the output goes from high to low when the switch closes. To the right it goes from low to high voltage.

4.4 The acousto-optic modulator

An acousto-optic modulator, AOM, uses the fact that a light beam can be diffracted on an acoustic wave inside a medium. An AOM consists of a piezo-electric transducer bonded to a crystal. When an electric radio frequency, RF, signal is applied to the transducer a mechanical strain is generated inside it. The mechanical strain will then travel through the crystal as an acoustic wave. The wave will act as a grating for the light. The wavelength of the acoustic wave depends on the frequency of the applied RF-signal. Acousto-optic devices in general are described in more detail in Ref. [14].

Depending on the acoustic wavelength, Λ , compared to the wavelength of the light, λ_0 , there are different kinds of diffraction. If

$$\frac{2\pi\lambda_0 L}{n\Lambda^2} \gg 1$$

the interaction, between the light and the acoustic wave, is said to be in the Bragg regime. The diffraction can be seen in Figure 4-2. L is the length of the acoustic wave and n is the refractive index.

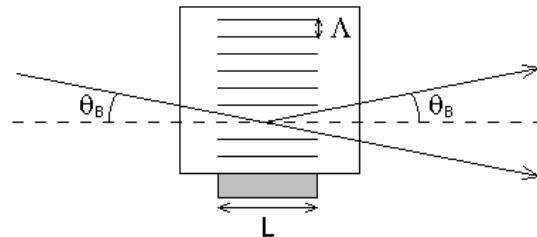


Figure 4-2: The diffraction of the beam inside an acousto-optic crystal. θ_B is the Bragg angle, L is the length of the acoustic wave and Λ is the wavelength of the acoustic wave.

When the light is incident at a certain angle, the Bragg angle θ_B , there will be only one order of diffraction. This is because except for the forward direction the light will only interfere constructively in that one direction. If the incident and the diffracted beam experience the same refractive index, the interaction is said to be isotropic. In this case the Bragg angle is given by

$$\theta_B = \frac{\lambda_0 f_a}{2nv}$$

where f_a is the frequency of the acoustic wave, and v is its velocity. The angle between the zero and first order will be twice the Bragg angle. The efficiency of the AOM will decrease rapidly as the angle is changed just slightly from the Bragg angle. The efficiency is given by the intensity in the first order divided by the intensity of the incident beam. It depends on the power, P , of the RF-signal as

$$\frac{I_1}{I_0} = \sin^2 \sqrt{\text{const} \cdot \frac{M \cdot P}{\lambda_0^2}}$$

The constant depends on the acoustic wave dimensions. λ_0 is the wavelength of the light and M is the acoustic-optic figure of merit for the crystal. A typical efficiency curve versus RF-power for a crystal can be seen in Figure 4-3.

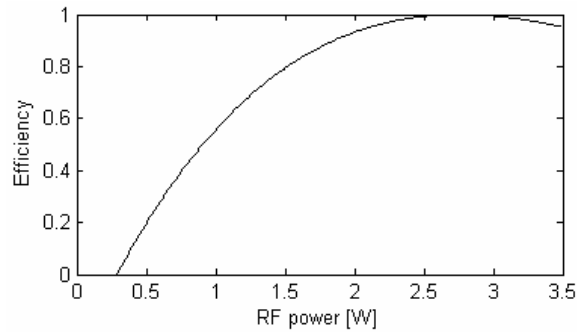


Figure 4-3: Efficiency versus RF-power for a typical acousto-optic modulator.

The extinction ratio for an AOM is defined in the same way as for an EOM. It informs about how much light that leaks through, in the direction of the diffracted beam, when no RF-field is applied to the crystal. To get a good suppression, the beam should be aligned such that reflections and scattered light inside the crystal are minimised.

The rise time of an AOM is given by the time it takes for the acoustic beam to travel through the light beam. The more the light beam is focused the faster the modulator becomes. But if the beam is focused too hard, it will not be small throughout the whole acoustic wave. It is also a problem that the outer part of the beam and the middle part of the beam will propagate at slightly different angles toward the focus, if the beam is focused too hard. Then only the middle part will fulfil the condition of the Bragg angle. The light beam should also pass the crystal close to the piezo-electric transducer to get a fast response. It is there that the quality of the acoustic wave should be the best.

When an AOM is used, it is also important how the crystal is oriented in the direction perpendicular to the one that sets the Bragg angle. In this other direction it should be oriented so that the light comes in close to the Brewster angle. In this way the losses in the surface, due to reflections, will be minimised.

The AOM used in the experiments were a Model 7200 Cavity Dumper from Coherent. This cavity dumper is constructed for use inside a cavity of a Picosecond dye laser system. It then enables a selective repetition rate of the output pulses. In the experiments here it was instead used as an ordinary modulator, with the beam just passing once through the crystal. It consists of two units, the 7210 Cavity Dumper Head and 7211 Cavity Dumper Driver. The crystal used in the Cavity Dumper Head is a SiO₂ Cavity Dumper, Model H-101, from Harris. Some specifications of the crystal are a rise time of less than 8 ns and an extinction ratio of 500:1. The diffraction efficiency is 15-20 percent for single pass, at the wavelength 514,5 nm. The frequency of the radio frequency field, from the driver, is 380 MHz. The maximum allowed power of the RF-signal in continuous wave mode is 1 watt. In pulsed mode the maximum allowed peak power is 10 W, as long as the average power do not exceed 1 W. It is recommended to stay well below both these limits. Besides the Coherent Driver, an Arbitrary Waveform Generator, AWG 520, from Sony Tektronix were used to drive the RF-field. It had a

resolution of 1 GS/s. A Mini-Circuits Amplifier LZY-1 was used, together with a DC Power Supply PS3010 from HQ Power, to amplify the RF-signal.

4.5 Electrical equipment

Attenuators of electrical signals were used in the experiments. Attenuation, as well as amplification, is often expressed in dB.

$$\text{Attenuation in dB} = 10 \cdot \log\left(\frac{P_{in}}{P_{out}}\right)$$

where P_{in} and P_{out} is the power in and out of the attenuator. There is also attenuation, of approximately -0.3 dB/m, in the coaxial cables used. To suppress reflections in the cables a resistance of 50Ω is normally put parallel to the signal, at the end of the cables.

4.6 Additional optical components

Several different optical components were use in the experimental set-up. Lenses of different focal lengths, mirrors for infrared light and apertures were used for the alignment. A pinhole of diameter $50 \mu\text{m}$ and a Newport F-SV single-mode fibre were tested in order to see whether they could improve the spatial cross section, of the laser beam. The fibre had a core diameter of $4 \mu\text{m}$. To picture the beam cross section a 3ComHomeConnect CCD-camera was used. $\lambda/2$ -plates and $\lambda/4$ -plates were used to manipulate the polarisation of the light. Rotated at a certain angle, a $\lambda/2$ -plate will turn the polarisation, of linearly polarised light, by 90° . A $\lambda/4$ -plate will make linearly polarised light circular polarised, if rotated at a certain angle. It can make the light either right-hand or left-hand circular polarised depending on how it is rotated.

4.7 The cell and the heating

The cell used in the experiment is cylindrical, and comes from Toptica Photonics. It is 2.5 cm long and has a diameter of 2.5 cm. On the sides there are thin optical surfaces. Inside the cell there is a natural composition of Rubidium.

To heat the cell two hairdryers were used. These were turned so that they blow on the optical surfaces of the cell. The optical surfaces have to be the warmest points of the cell. If this is not the case the non-vaporized Rubidium will stick to these surfaces. The temperature was regulated by changing the distance between the dryers and the cell. The temperature was measured with a thermoelement wire of NiCr-Ni, Type:K. It was placed at the point of the cell that was expected to be the coolest. It is the coolest point of the cell that sets the vapour pressure inside the whole cell. The resistance thought the thermoelement was measured with an ohmmeter. The resistance increases as the temperature increases.

4.8 The detection

For detection of light photodiodes and photomultiplier tubes can be used. A photodiode consists of a photosensitive cathode. Photons hitting the cathode will extract electrons from the surface. The electrons will be accelerated towards the anode by an electric field. The current from the electrons will be detected. A photomultiplier tube works almost in the same way. The electrons released from the cathode will be amplified on a series of dynodes. Each electron will extract a few more electrons from each dynode. In this way the signal is multiplied at every dynode. At the end of the tube the current will be detected. A photomultiplier tube can detect much less light than a photodiode because of the amplification. However, noise will be generated in the amplification process. This will lead to a higher noise level than for the photodiode. Therefore it is not advantageous to use a photomultiplier if the signal is weak compared to the noise level. Weak signals can only be detected, in a photomultiplier or

a photodiode, if the noise is even weaker. To reduce the noise the tube can be cooled and screened from surrounding light. More information on the noise in a photomultiplier tube can be found in Ref. [15].

The photo-diode used in the experiments was an ET2010 from Electro-Optics Technology. It has a sensitivity of 0.4 A/W at 830 nm. From the sensitivity curve it can be seen that the sensitivity is almost the same at 795 nm. The rise time is less than 1 ns. The photomultiplier tube used was a Hamamatsu R943-02. It has a rise time of 3.0 ns and a transit time through the tube of 23 ns. A typical sensitivity is $3.6 \cdot 10^4$ A/W depending on the operation voltage. The tube has a normal anode to cathode supply voltage of 1500 V. It has to be operated at a lower voltage when there is much light in the signal, or in the background. The average anode current should not exceed 1 μ A. The voltage to the multiplier was taken from a Fluke 412B High Voltage Power Supply.

The signals from both the photodiode and the multiplier tube were detected on a Tektronix TDS 540 Digital oscilloscope. Also other electrical signals were studied at this oscilloscope. It has a sampling rate of 1 GS/s. For both the photodiode and the photomultiplier, it is important that the cable to the oscilloscope is well screened. If a screened cable is used, the noise from the surrounding will not interfere as much with the signal. To measure the power in the beam during alignment a LM-2 Coherent power meter, connected to a FM Coherent Fieldmaster, was used.

Chapter 5

Experimental procedure and results

In the plan for this master's thesis a lot of experiments were included. The final goal was to achieve high efficiency photon echoes with counter propagating beams. However, the initial experimental steps demanded much more work than expected from the beginning. Just to generate light pulses of the right length, which was the first step, took up a lot of time in this master's thesis project. A reason for that was that the photon echo group has not previously worked on such short time scales, which was required for these experiments. Normally work done in the group is on time scales ten to hundred times longer. The equipment available is therefore not suited right away, for the purposes it is used for here.

5.1 Generating a short pulse

To be able to perform the photon echo experiments in rubidium, short light pulses have to be used. Every pulse should have a duration of somewhere between 5 and 10 ns. It has to be this short because the lifetime of rubidium is around 30 ns. This means that the echo will be much weaker if it comes later than 30 ns after the first pulse. For both the pulses and the echo, in a two-pulse echo, to fit within 30 ns the pulses cannot have too long durations. It must be possible to distinguish the pulses and the echo. On the other hand the pulses cannot be too short either. For a shorter pulse it will be harder to achieve a high enough pulse area, since the power out from the laser is limited. Another reason for the pulses not to be short is that they then will have a larger bandwidth. If the bandwidth is too large the light will cover more than one transition, and the experiment will be ruined. The separation between the hyperfine levels in the excited state in rubidium is 817 MHz. For a pulse with a Gaussian shaped intensity distribution over time, the minimum full width half maximum, FWHM, of the pulse is given by [16]:

$$\Delta\tau = \frac{2 \cdot \ln 2}{\pi \cdot \Delta\nu}$$

where $\Delta\nu$ is the bandwidth of the pulse. It can be calculated that the pulse should be much longer than 0.54 ns, in order not to overlap the closest transition. Since it is desirable to have a small bandwidth of the pulse, the pulse should be close to transform limited. A transform-limited pulse has a bandwidth that is the smallest possible for its pulse length, given by the expression above. Another important aspect in the pulse generation is that, there should not be much light before and after the pulse. This sets rather hard requirements on the extinction ratio, and on the transient behaviour after the pulse.

5.1.1 Generating a pulse with EOMs

The first idea, how to generate short pulses, was to use electro optical modulators, EOMs. Because the high voltage switches only have a fast rise time, but not a fast turn-off time, more than one switch had to be used. Two EOMs, with one switch controlling each one of them, could be used. Then one of the modulators would turn on the light, and the other would turn it off. The high voltage would be put on one of the plates inside each modulator and the other plate would be connected to ground. Another way, which was also tried, is to use only one EOM with a switch coupled to each one of the two plates inside the modulator. First a high voltage is applied to one of the plates, and a field over the crystal is created. Then a voltage of the same magnitude is applied to the other plate. The field is now turned off again, since the voltage is the same on both the plates. The result is the same as if no voltage was

applied to any of the plates. Results from both methods will be given below. First however the losses, the extinction and the response of a single EOM are studied.

To find the half-wave voltage, the polarisers before and after the EOM were rotated to block the light, when no field is present over the EOM. Maximum signal through is achieved when the crystal is rotated with the correct angle and the voltage over the EOM is equal to the half-wave voltage. By rotating the crystal and changing the voltage for each angle the half-wave voltage was found to be 257 V. The EOM was locked in the position where the maximum signal was achieved. The intensity, without a voltage applied across the EOM, turned out to be rather high. A reason for this might be that the EOM is turning the polarisation to some extent even without a field. If the light out from the EOM is slightly elliptical polarised it will be impossible to extinguish it by the last polariser. To overcome this problem a $\lambda/4$ -plate can be placed between the EOM and the polariser. By turning the plate to a certain angle it can modulate any elliptical polarised light to linearly polarised light. The extinction of the light was improved when the $\lambda/4$ -plate was introduced. Some measurements made, with and without the plate, are found in Table 5-1.

Without EOM (with polarisers rotated to let the light through)	10.5 mW
EOM with 257 V	8.52 mW
EOM with 0 V	140 μ W
EOM with 257 V and $\lambda/4$	8.18 mW
EOM with 0 V and $\lambda/4$	39 μ W
Background	1.1 μ W

Table 5-1: Measurements of the power after the EOM and the polariser under different conditions.

From the above results the losses with only the EOM were calculated to be

$$\frac{I_0 - I_{EOM}}{I_0} = \frac{P_0 - P_{EOM}}{P_0} = \frac{(10.5 - 8.52) \cdot 10^{-3}}{10.5 \cdot 10^{-3} - 1.1 \cdot 10^{-6}} = 19\%$$

with the background subtracted. The extinction ratio, for the case with only the EOM, was calculated to be

$$\frac{I_{0V}}{I_{257V} - I_{0V}} = \frac{(140 - 1.1) \cdot 10^{-6}}{8.52 \cdot 10^{-3} - 140 \cdot 10^{-6}} = 1.7\% = \frac{1}{60}$$

With the $\lambda/4$ -plate the losses were 22 %, and the extinction ratio was 1/215. It is a good choice to use a $\lambda/4$ -plate together with the modulator, since the extinction ratio is improved. This is of greater importance than the increased losses when a plate is used.

A switch was now connected to the EOM to study the response of the light upon switching. The light was detected with the photodiode to see the fast events. It turned out that the signal had a fast rise time, but there were transient oscillations after the switching. By studying the signal from the switch, directly connected to the oscilloscope with a probe, the same behaviour as in the light was observed. Therefore it could most definitely be said that the oscillations is not due to the EOM, but to the switch. Decreasing the speed of the switch could reduce the oscillations. In Figure 5-1 the light turned on by a switch, where the resistance in series with the output has been changed between the measurements, is shown. In the three curves, from the top to the bottom in the figure, the total resistance on the output is 16 Ω , 26 Ω and 34 Ω . It can clearly be seen that the oscillations after the switching is reduced as the resistance is increased. The rise time however is increased. For the three measurements from top to bottom the rise time is measured to be 6 ns, 7 ns and 10 ns. As the switch becomes slower the oscillations are reduced. This is not a solution however, since a fast response of the switch is needed.

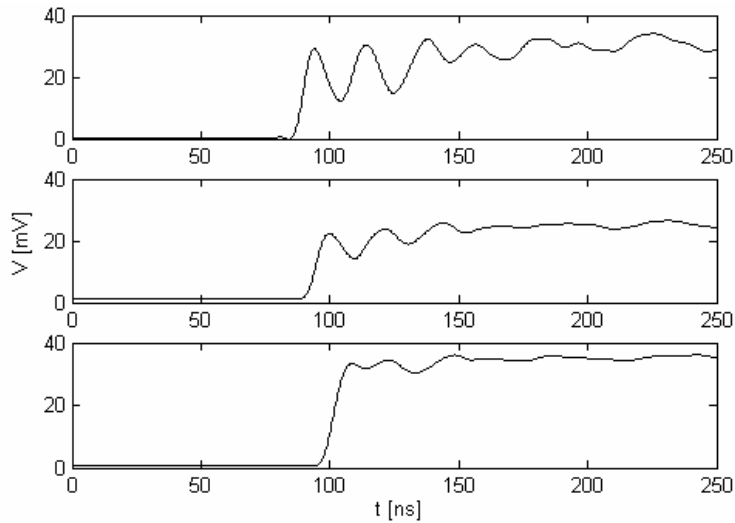


Figure 5-1: The light signal from an EOM, with different resistance on the output of the switch.

In Figure 5-2 signals of the light after an EOM is shown, for cases when the switch is coupled in different ways. The two configurations are the ones described earlier in Figure 4-1. The signal in the first picture comes from a switch that turns from high to low voltage, and the second comes from a switch that turns from low to high voltage. The resistance is almost the same for the two cases, 26Ω respectively 28Ω . The reason why the signal in the top picture is smaller, and the extinction worse, is that the EOM was not aligned as well when this signal was collected. Besides this the oscillations are similar. Therefore the conclusion can be drawn, that the coupling of the switch does not make a considerable difference. The rise time is around 8 ns in both cases. In the continuation the switches will be coupled as in the picture at the bottom.

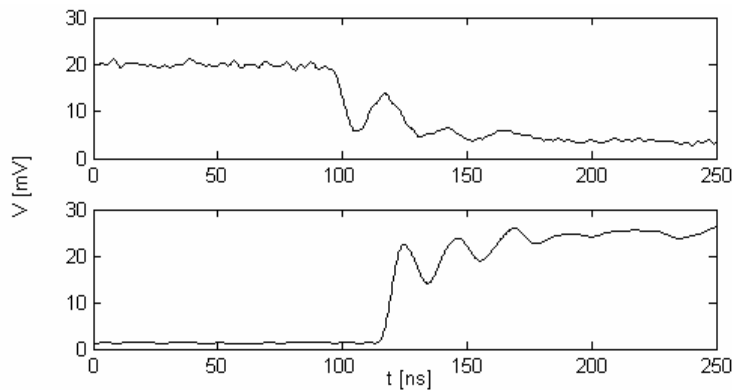


Figure 5-2: The light response signal from an EOM, with two different electrical configurations of their switches (compare Figure 4-1).

Two switches were now used together with only one EOM. The switches with slightly different response, shown in the two top pictures in Figure 5-3, were connected to each one of the plates inside the EOM. From the signals collected, for each one of the EOMs, a simulation of how the pulse would look was done. The electrical signal to either one of the switches was calculated, from the measured signal of the light. Applying these signals to the two plates in the EOM, and looking at the difference in voltage, a simulation of how the corresponding light would look like was done. The result can be seen in the third picture in Figure 5-3. The measurement of the real signal of the pulse is given in the last picture. The switches were located in the same position in time, as the above pictures indicate. It can be seen that the real pulse has a longer duration than the simulated pulse. The simulated pulse was made under the assumption that the plates did not affect each other. This is probably not true, since neither of the sides is connected to the stable ground. Therefore the difference in the two pulses. The

duration of the real pulse was approximately 13 ns FWHM. The pulse could not be made shorter by moving the two switches, without decreasing the intensity. The oscillations in the separate switches are affecting the generation of the pulse, which can also be seen in the picture. After the pulse there are oscillations, and it takes rather long time until they have faded away. No matter how the switches were moved in relation to one another, it was not possible to cancel the oscillations after the pulse.

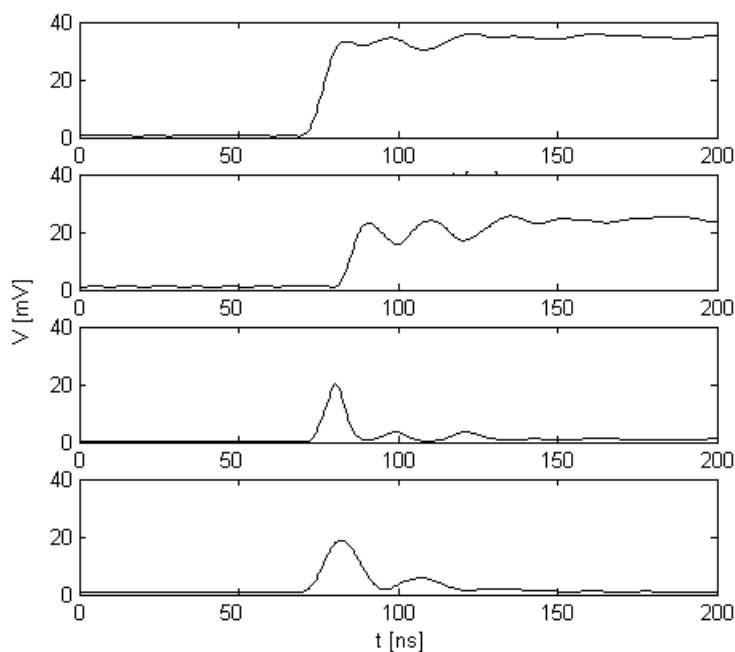


Figure 5-3: The top two curves show the response of the light from the two EOMs. From these two functions a simulated pulse has been calculated, seen in the third figure from the top. At the bottom the real result is shown when both the switches are connected to one EOM, switching at the same times as above.

Since the plates inside the EOM affected each other when neither one of them are connected to ground, a set-up with two EOMs were tried instead. There are two ways of generating the pulse with two EOMs in a row. One of them is with a polariser between the modulators, and one is without a polariser. In both cases there are polarisers placed before and after both the EOMs. In the first case, the first EOM turns on the light by letting it through the middle polariser. Then the last EOM turns it off by rotating the light so that the last polariser cancels it. In the other set-up, without a polariser in the middle, the EOMs are placed so that they will rotate the light in the opposite direction from one another. In this way it is hoped for that the oscillations will cancel each other.

In Figure 5-4 the results from both methods have been collected. The time separation between the EOMs is decreasing in the pictures from top to bottom. For the case with a polariser in the middle, the pulse duration decreases when the time separation between the switches decreases. However the intensity of the pulse is also decreasing, which is not desirable. It can be seen that the alignment without the additional polariser, do cancel most of the oscillations. However the pulse duration for this case is larger than for the other alignment. With the polariser between the EOMs it is possible to do short pulses. Even if the pulses can be made short with this arrangement, there is however a lot of light coming through after the pulse. Therefore neither of the arrangements are good enough. Another way of generating the pulse has to be found.

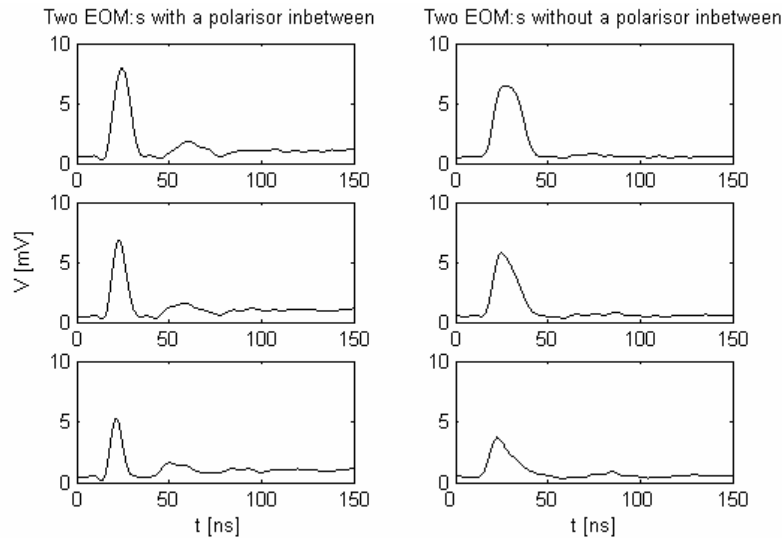


Figure 5-4: Pulses of light generated by two EOMs, with and without a polariser between the modulators. From the top to the bottom the time separation between the two EOMs is decreasing.

5.1.2 Generating a pulse with an AOM

Since the EOMs did not give good results in generating pulses, an AOM was instead tried. Most AOMs are much slower than what is required here. A cavity dumper AOM was however found that should be fast enough. The AOM was set up, and a concave mirror of focal length 7 cm focused the beam onto it. The RF-signal came from the Coherent drive unit. After the crystal an aperture was placed to distinguish the diffracted beam from the incident beam. The intensity in the diffracted beam was measured with and without a continuous RF-field applied to the crystal. This measurement was done after the aperture. The intensity in the zero order beam, after the crystal, was also measured with the RF-signal turned off. The background was measured and subtracted from the other measurements.

The efficiency turned out to be low and the suppression was not good. It is hard to adjust the crystal, and the beam onto it, trying to achieve an optimum. It is also hard to place the aperture in the right place and making the hole the right size. However these were probably not the main reasons, for not achieving a higher efficiency and a lower extinction ratio. The beam from the diode laser does not have a nice symmetrical spatial cross section. Therefore the focus also becomes irregular, and there will be a lot of scattered light around the focus. Pictures of the beam and the focus were taken with the CCD-camera. These pictures can be seen in Figure 5-5. The picture of the beam, to the left, shows that the cross-section is very irregular. Most of the intensity in the beam is located in the mode to the left in the picture. A lens of focal length 1 m achieved the focal spot photographed, to the right in the figure. The photo was taken 150 cm after the lens, showing that the beam was quite divergent before the lens. It is not possible to see the irregularities in the focal spot, or the spread light around the focus. It can however be seen that the focus is longer in the vertical direction than in the horizontal. Some of the light in the lower part of the beam is probably reflected at the bottom of the crystal, leading to the high extinction ratio.



Figure 5-5: Photographs taken by a CCD-camera: The beam cross-section to the left and the focus of the beam to the right.

To clean up the beam an attempt to focus the beam onto a fibre was made. There was no success in getting much light through the fibre. This is partly due to that the loss in the fibre increase when the wavelength of the light increases above the normal operation range. Then the transmittance will easily be affected by bending of the fibre. To minimize this effect the fibre was kept as straight as possible. However, the main reason for only getting through a little amount of light is probably that the focusing again is not good enough. It is very important that the light is focused onto the core of the fibre, which only had a diameter of 4 μm . Instead of the fibre another method for cleaning up the beam was tried. The beam was focused onto a pinhole of diameter 50 μm , with a 5 cm lens. Now most of the light came through. Around 18 % of the light was lost. It is the outermost parts of the focus that were blocked. These are also the parts giving rise to most of the scattered light in the crystal. The efficiency and the extinction were improved by the pinhole, so it was left in the experimental set-up.

A telescope set up by lenses varied the size of the beam, onto the focusing mirror before the crystal. If the beam is too large the outer parts of it will not fulfil the condition for the Bragg angle. These are focused with another angle than the middle part of the beam. On the other hand, if the beam is smaller the size of the focus will be bigger. This will lead to a slower rise time of the crystal and more scattered light. A size that was good was found and the measurements in Table 5-1 were collected.

Total intensity after AOM	21.4 mW
Background to the total intensity measurement	430 nW
Diffracted beam with the RF-field turned on	562 μW
Diffracted beam with the RF-field turned off	3.07 μW
Background to the diffracted beam measurements	950 nW

Table 5-2: Measurements after the AOM, with a continuous RF-field turned on and off.

From these results the efficiency is calculated to 2.6 %, as shown below. Here the losses in the crystal are not included in the efficiency expression, as it was in the expression given in the section about AOMs in chapter 4.

$$\frac{I_1}{I_0} = \frac{P_1}{P_0} = \frac{(562 - 3.07) \cdot 10^{-6}}{21.4 \cdot 10^{-3} - 430 \cdot 10^{-9}} = 2.6\%$$

The extinction ratio is calculated to 260:1, from the measured values above.

$$\frac{I_{noRF}}{I_{withRF}} = \frac{P_{noRF}}{P_{withRF}} = \frac{(3.07 - 0.95) \cdot 10^{-6}}{(562 - 3.07) \cdot 10^{-6}} = 0.38\% \approx \frac{1}{260}$$

The continuous RF-signal, from the Coherent drive unit, can be seen to the left in Figure 5-6. The detected signal was measured to 3.66 V peak-to-peak, and the effective value was 1.24 V according to the oscilloscope. The effective value of the sinusoidal signal, U_{RMS} , could otherwise be calculated as the root mean square of the peak-to-peak value, U_{pp} .

$$U_{RMS} = \frac{U_{pp}}{2\sqrt{2}}$$

The power, P, is related to the effective value of the voltage as

$$P = \frac{U_{RMS}^2}{R}$$

When the measurement was done the resistance, R, inside the oscilloscope was 50 Ω . There were also attenuators of totally 12 dB coupled in series with of the signal, when it was detected. As the signal is coupled to the crystal instead no attenuation will be used. From the formula in section 4.5 the power into the attenuators can be related to the power out of them as

$$P_{in} = P_{out} \cdot 10^{12/10}$$

The cable used was of the same length as the cable going to the crystal, when it is connected instead of the oscilloscope. Therefore the attenuation of the cable can be disregarded. From the measured values above, the power going into the crystal is calculated to be 0.5 W in the continuous mode.

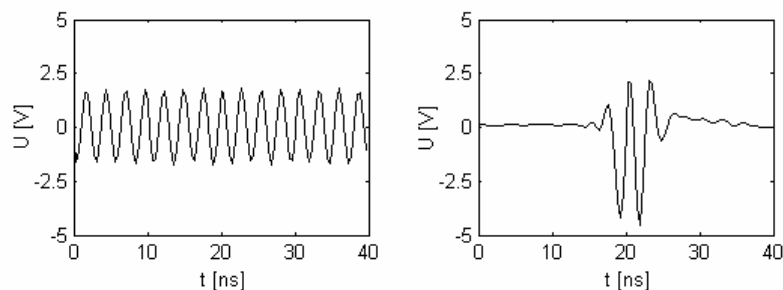


Figure 5-6: Signals from the RF-field studied on the oscilloscope. To the left the continuous RF-field is shown. To the right a pulse out from the Coherent drive unit is studied.

To the right in Figure 5-6 the RF-field for a pulse is shown. The peak-to-peak value here was 6.7 V and the effective value was 2.4 V at the top of the pulse. From this the peak power 1.8 W is calculated in the same way as above. To achieve a higher RF-power an amplifier is used. The amplification in it was approximately 40 dB. Changing the attenuation put in series with the amplifier the power can be varied. The power of the light is measured, with the powermeter, as the power of the RF-signal is varied. The measurements, for pulsed mode, are given in Table 5-2. The values of the power into the crystal, in the third column, are calculated from the voltage in the second column.

Attenuation [dB]	$U_{\text{oscilloscope}}$ [mV]	P_{RF} [W]	P_{light} [μW]
39	1.7	7.3	122
40	1.4	5.8	100
41	1.26	4.6	90
42	1.06	3.7	76
43	0.88	2.9	63
44	0.76	2.3	54
45	0.62	1.8	44

Table 5-3: Measurements of the light in the diffracted beam, for different powers of the RF-field into the AOM-crystal.

The result of the measurements can be seen in the graph in Figure 5-7. The points in the graph follow close to a straight line. The graph can be compared to the curve in Figure 4-3. The measured results seem to be within the almost linear part of the efficiency curve.

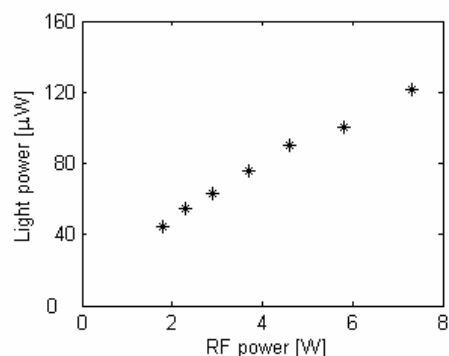


Figure 5-7: Measured light power versus the power of the RF-field into the AOM.

With the Coherent drive unit it is not possible to change the length of the RF-pulse. It can only generate pulses of equal length at a given repetition rate. It is not possible to make two pulses shortly after one another. Therefore the Arbitrary waveform generator was used instead. With the AWG it is

possible to generate an electric signal with any shape preferred. In figure 5-8 the two RF-drivers are compared. On top the RF-signals are shown. These are adjusted so that the amplitude will be the same from both the drivers. It can be seen that the Coherent driver does not give a pulse centred at zero field. This however does not seem to affect the result in the light pulse. The light pulses can be seen in the lower part of the figure. The two light pulses, from the different drive units, are very similar. This means that using the AWG instead of the Coherent drive unit will not affect the results negatively. By changing the duration of the RF-field from the AWG, the duration of the light pulse can be changed. There is a limit however of how short the light pulse can be, set by the crystal. Even if the RF-pulse is made shorter than what is shown in the figure, the light pulse will not become shorter. The pulse duration was measured to be somewhere between 9.9 and 10.2 ns FWHM, for the AWG.

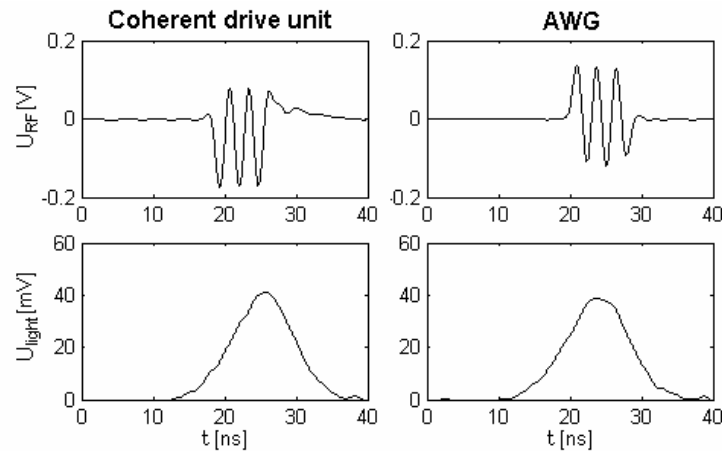


Figure 5-8: Comparison between the Coherent Drive unit and the AWG. On top the RF-pulses are compared and at the bottom the corresponding light pulses are shown.

By making the RF-pulses a little longer a higher efficiency were achieved. The RF-frequency was also changed a bit from its value 380 MHz, to look for changes in the efficiency⁵. The best result achieved is shown on top of Figure 5-9. The frequency was 365 MHz, but the results were almost as good at 380 MHz. The peak voltage of the pulse in the upper part of the figure is 77 mV. This corresponds to a light power of 3.9 mW at top of the pulse. After the AOM the total power, without an RF-field, were measured with the powermeter to be 19 mW. The leakage through in the diffracted order, without the RF-field, was measured to be 2.8 μ W. From these measurements the efficiency at top of a pulse was calculated to be 20 %. The pulse duration is around 10 ns FWHM.

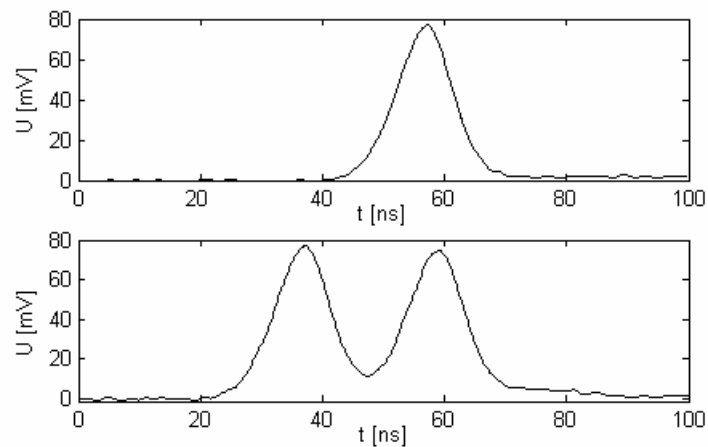


Figure 5-9: On top the best light pulse achieve with the AOM and the AWG is shown. At the bottom two consecutive pulses are shown, with the separation needed to distinguish them.

⁵ One has to be careful when changing the frequency however. The attenuation in the cables is reduced when the frequency is decreased. This might lead to a too high power into the crystal, with the other settings unchanged.

At the bottom of Figure 5-9 two pulses generated by the AOM and the AWG are shown. The separation between them is 22 ns. If they are brought closer together the intensity will not drop far in between the pulses, before it goes up again. This will be a problem when the pulses are going to be used in the experiments. The separation now showed is longer than desired, but it is more important to be able to distinguish the pulses.

5.2 Finding Rubidium absorption peaks

The next step in the experimental work was to look for absorption in the Rubidium cell. The cell was placed in a holder in the beam path. To find absorption peaks in rubidium at room temperature a sensitive measurement method is needed. The transmitted signal was studied, as the laser frequency was tuned back and forth, over a small interval. The modulation of the laser frequency was over about 1 GHz, and it was a sinus modulation. This modulation corresponds to an electrical signal to the EOM, inside the laser, of 80 V peak to peak. The centre frequency was changed, and the modulation of the signal was studied as a function of the wavelength. The wavelength was measured at the same time by the Burleigh wavemeter. The Fourier transform of the signal was studied at the oscilloscope. The modulation frequency was 13.3 kHz. One reason for this choice was that this frequency is far away from the low frequency noise in the background. It is also chosen as an odd number not to interfere with the sampling frequency of the oscilloscope.

A peak could be seen in the Fourier transform at the modulation frequency, at all wavelengths. This is due to the fact that the laser intensity varies as a function of the wavelength. Some changes in the peak at the modulation frequency could be seen as the wavelength changed. If the centre wavelength of the modulation is located at one side of an absorption peak, there will be an increase in the modulation frequency peak on the oscilloscope. When the wavelength is modulated back and forth just on top of an absorption peak, there will be a modulation of the signal with twice the modulation frequency. The two different modulation intervals are shown in Figure 5-10. This is a very sensitive measurement method to make sure whether on a top of an absorption peak or not. There will be no signal peak at the double modulation frequency in the Fourier transform unless the wavelength is located at an absorption peak. This is true as long as no mode-hops occur in the laser frequency. It could easily be confirmed that so is not the case.

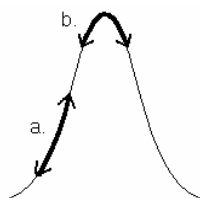


Figure 5-10: Modulation of the laser frequency at the position a. gives a modulation of the signal at the modulation frequency, and at the position b. it gives a modulation at twice the modulation frequency.

Using the method described above four peaks in the D1-line was found. Looking at the cell at the same time as the frequency were tuned back and forth over a top with a low modulation frequency, fluorescence could be seen. This confirmed that there were actually absorption peaks at the locations found. The locations of the peaks and the modulation signal strengths can be seen in Table 5-4. The strength of the modulation signal can just give a hint of the strengths of the actual absorption peak, and is not an exact measurement.

λ [nm]	Signal at $2\omega_{\text{modulation}}$ [μV]
794.7501	21.6
794.7553	70.4
794.7622	102.0
794.7653	31.6

Table 5-4: Measurements made of the signal on the oscilloscope, at the double modulation frequency in the Fourier transform. Absorption peaks were found at the wavelengths given.

By comparing the result to a known absorption spectrum [17] the peaks could be identified. The two strong peaks in the middle come from the ^{85}Rb isotope. The peak at 794.7501 nm is from ^{87}Rb and corresponds to transitions from the level $F = 1$. This peak consists of two hyperfine transitions, not resolved by this measurement technique. The transitions are $F = 1$ to $F' = 2$, which has the lowest wavelength, and $F = 1$ to $F' = 1$. The peak at 794.7653 nm is the transition from the other hyperfine level in the ground state. Here the transitions $F = 2$ to $F' = 2$ and $F = 2$ to $F' = 1$, cannot be resolved. These two peaks are separated by 817 MHz, as are also the two peaks from $F = 1$ described above. The Doppler linewidth is approximately 500 MHz FWHM at room temperature, calculated from the formula in Appendix A. Therefore the peaks will overlap in frequency and they cannot be resolved.

When the measurements above were made the AOM was in continuous wave mode. In this mode the absorption is very weak. This is due to the fact that when the laser is set to a transition from the $F = 1$ state in the ground state, the atoms will be pumped over to the $F = 2$ state in the ground state. From there they cannot be excited again, because the bandwidth of the laser is much smaller than the separation between the two hyperfine states in the ground state. This pumping occurs rather fast because there are not many atoms in the cell, compared to the number of photons in the beam. The absorption seen is therefore mostly due to the atoms entering the beam from the sides. These atoms have not yet been excited. In the same way the atoms are pumped over to the $F = 1$ state when the laser is set to the $F = 2$ transition. To see more absorption the laser could be run in pulsed mode, with low repetition rate. If the repetition rate is low enough, there would be enough time between the pulses, for most of the atoms to relax back to both hyperfine levels. It was possible to find the peaks with continuous laser light in the measurement above, because the method used there is very sensitive. To collect absorption spectra on the other hand, it is hard to see anything unless the absorption is increased.

An attempt to collect an absorption spectra was made with pulses. To increase the absorption further the cell was heated. The two hairdryers was put on each side of the cell. The thermoelement was placed on the point of the cell where the lowest temperature was found. The absorption was measured at different frequencies. The laser frequency were changed by hand by changing the temperature and current through the diode. In this way it is hard to get a nice absorption spectra. The laser does mode-hops when tuned like this. Therefore it is difficult to collect information at some wavelengths. Also the wavemeter drift some in time, not showing the right wavelength. It can easily be calibrated, but it takes some time to do between each measurement, since a lot of points are to be collected. Not enough measurements were made to get an absorption spectra. A spectra could be achieved if more time were to be put on this. It is however not of any importance to the continuation of the experimental work to be carried out here, and therefore it is not done.

5.3 Detecting an echo

Before any attempts to detect an echo were made, an estimation of how strong the echo signal would be was made. For that purpose some measurements were needed. A rough estimation of the beam radius was made by measuring the power in the beam, as different parts of it were blocked. A razorblade was inserted into the beam from one side. It was gradually moved blocking the beam more and more and from the measured power at the different positions, an estimation of the beam spot size was made, to be 0.5 mm. The peak power of the pulse before the cell was measured to be around 450 μW . This was done by measuring the power of continuous light with the powermeter and then comparing the signals from the photodiode, for the two cases. The temperature in the cell was approximately 59 $^{\circ}\text{C}$. A calculation of how many photons there is supposed to be in a two-pulse echo, under the conditions given above, is done in Appendix B. In this calculation the absorption of the echo, on its way out of the sample, is not included. The echo will therefore be weaker than what is calculated in the appendix.

To detect the echo signal a photomultiplier tube was set up. To distinguish the echo from the excitation pulses, an EOM was placed in front of the detector to open just before the echo came

through. The excitation pulses on the other hand were blocked. Some of the light from the pulses would however leak through. Another EOM was placed after the AOM to suppress the light after the pulses. This EOM was set to let the pulses through and then shut right after they had passed. This EOM would reduce the light after the pulses, but there would still be some leaking through. Some peaks in the light after the pulses could be due to reflections of the RF-signal in the cables. To suppress these reflections attenuators were placed, both between the AWG and the amplifier and between the amplifier and the crystal. The power from the AWG was increased to compensate for the attenuation. The reflections would however be attenuated more than the signal, since they pass the attenuators more times. The two EOMs introduced in the set-up will have oscillations, as seen before when they were used trying to generate light pulse. However, the intention was that the suppression they achieved would improve the signal more than the oscillations they introduced would damage it. The experimental arrangement to detect the photon echo can be seen in Figure 5-11.

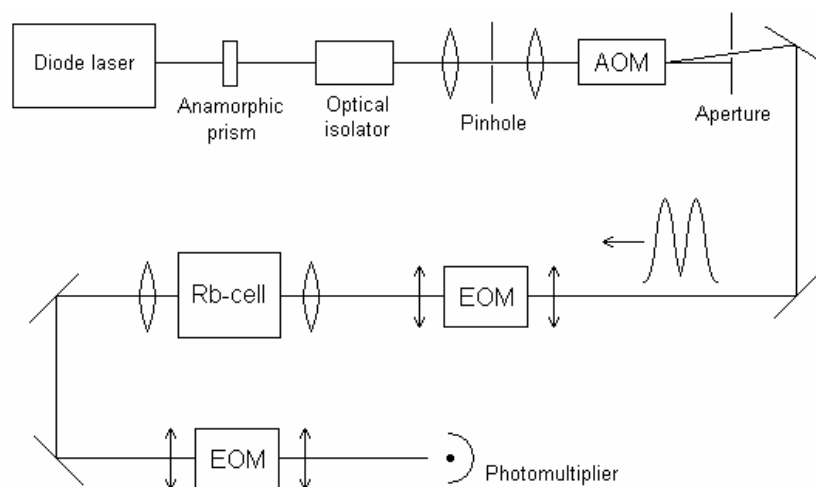


Figure 5-11: The experimental set-up for detection of a two-pulse photon echo. The two excitation pulses can be seen in the picture as well. AOM stands for acousto-optic modulator and EOM for electro-optic modulator. Lenses, mirrors and polarisers are also shown in the drawing.

The beam was focused in the cell to get a high intensity. A lens with a focal length of 15 cm was used for this purpose. To find the exact position of the focus, the CCD-camera was placed in the beam after the expected focus position. The beam cross section was studied, as a razorblade was moved slowly into the beam from one side. Depending on which side of the focus the blade entered the beam, the picture of the beam from the camera, was cut from different sides. By moving the razorblade position along the beam, always entering from the same side, the focal spot were found. The cell was placed so that the focal spot was positioned in its centre.

The average current from the photomultiplier was measured as the voltage across it was increased. This was done in order to make sure that the current did not exceed the maximum limit. It is desirable to have as high amplification as possible, and therefore the voltage is increased until the current limit is reached. The signal from the multiplier was then studied with the oscilloscope, and the two pulses were seen. The positions of the gates from the EOMs could also be observed. This was done by moving them as the signal was studied, to see how the pulses changed. The EOMs, the AWG and the oscilloscope were triggered from the digital pulse generator. All four trigger times could be moved independently. The repetition rate of the pulses from the AWG was 10 Hz.

When the pulses were studied with the photomultiplier they had a duration of 13.2 ns FWHM each. For comparison the photodiode was set up again. The pulse duration in the signal from the diode was 10.9 ns. It could be seen that fast events are extended in time in the multiplier. Since this effect is rather small, it would probably not affect the detection of the echo.

The peak intensity of the pulses when placed off resonance, without being blocked by the EOM-gates, corresponds to a signal of 397 mV on the oscilloscope. With the EOM-gates placed to block the pulses the peak signal was found to be 31 mV. This corresponds to an extinction ratio of 1/11 in the EOM for light that is pulsed. This is a lot worse than for the case when the light was continuous. The suppression could probably be improved if the EOM was aligned for the pulses, instead of for continuous light. This is however more complicated experimentally, and was therefore not done. When the EOM-gate was positioned to block the pulses the amplification in the photomultiplier could be increased. The peak signal then increased from 31 mV to 61 mV. If the echo is assumed to be one percent of the pulse intensity⁶, it should have a peak signal of

$$\frac{61}{31} \cdot (397 \cdot 0.01) = 7.8 \text{ mV}$$

when the amplification is increased.

In Figure 5-12 the signal from the photomultiplier can be seen. The amplification is the same as when the last measurement above was made. The EOM-gates are placed so that one suppresses the pulses and the other suppresses the background after the pulses, as described above. A lot of light from the pulses leaks through the EOM, as can be seen in the figure. The measured curves are zoomed in, to better see what happens after the pulses. The lower trace shows the signal with the frequency off resonance. It could be seen that there are some oscillations in the light after the pulses. By moving the EOM-gates slightly the oscillations can be changed. Minimum oscillations were achieved when the gates were positioned at the same places as when the signals in the figure were taken. The upper trace in the figure shows the signal close to resonance. When the frequency was positioned exactly at resonance the absorption was too high. Instead of changing the temperature, to find an absorption that is adequate, the frequency was changed slightly off resonance. The absorption was approximately 70 percent at the wavelength for which the signal in the figure was taken. It has been shown that the absorption should be close to 63 percent to achieve an as high as possible echo intensity. The absorption can be seen by comparing the signals, on and off resonance, in the figure. The scale of the upper curve is smaller than for the scale in the lower one.

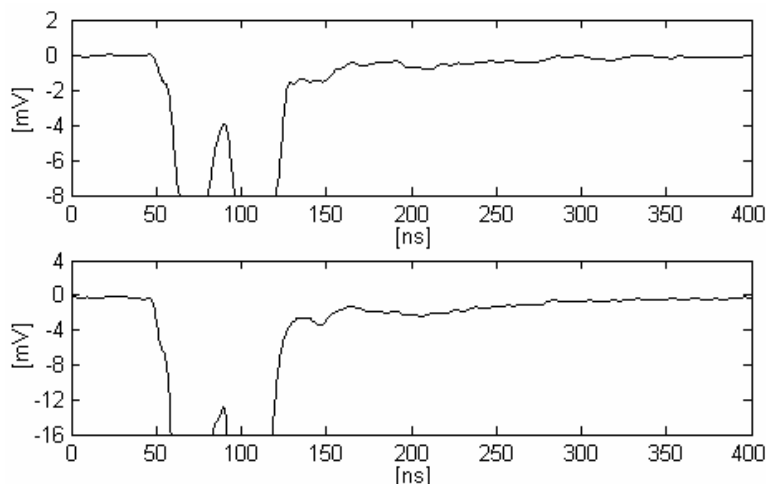


Figure 5-12: Signals from the photomultiplier. The signal after the two pulses is zoomed in. The top picture shows the signal close to resonance and the bottom picture is the signal off resonance.

When comparing the light after the pulses it can be seen that it looks slightly different for the two cases in Figure 5-12. However, when positioned at different positions within the absorption profile, the signals after the pulses were also different. No unambiguous conclusions regarding whether some of the light after the pulse is due to an echo, can therefore be drawn. From the estimation above the echo signal should be approximately 8 mV. It can be seen from the upper picture in the figure that

⁶ This assumption is not based on the results in Appendix B, but instead on what is known to be a normal value of the echo intensity if optimum excitation pulses are used.

such a high signal would easily be distinguishable. The background signal is approximately 2 mV after the pulses. The noise in the signal cannot be seen in the picture since the signal has been averaged over a few samplings shots. It was however measured to be approximately 1 mV. The minimum detectable signal is normally a signal that is as large as the noise level. Considering this limit an echo of 0.13 % could be detectable. However it might be hard to detect such a weak echo even if it is possible due to the noise limit. Since the oscillations after the pulses alter with the wavelength, it will be hard to distinguish the echo from the background.

It is hard to say if there is no echo at all or if there is an echo that is too weak to be detected. A lot of things can be wrong in either the experimental set-up or in the assumptions made. Maybe the echo is much weaker than one percent of the pulse intensity. The time separation between the first pulse and where the echo should come is 44 ns. If this is compared to the lifetime of the excited state, which is 28 ns, it could be understood that the echo will be weak. Another reason for the echo to be weak is that the temperature was increased to achieve higher atom density in the sample, than was calculated in Appendix A. This was done because there were many more photons in the pulse than atoms in the sample. By increasing the temperature, an absorption of the pulses that was adequate was found. The echo however will not contain as many photons as the pulses. The absorption of the echo may therefore be higher than for the pulses. By reducing the intensity in the pulses, instead of increasing the temperature, the absorption of the echo would be more similar to the absorption of the pulses. For that case the atom density would set the absorption instead of the number of photons in the pulse. However the intensity of the echo is reduced when the pulse intensity is reduced. This could be investigated further by calculations, to see if the result could be improved by reducing the pulse power.

The experimental set-up in the laboratory can be seen in Figure 5-13. This is the same optical set-up as illustrated in Figure 5-11, but with some additional components. A small part of the beam is led off to the wavemeter, the white box to the left in the picture, to measure the wavelength. The red box to the right in the picture is the laser. On the upper table some drive units are placed. In Figure 5-14 the Rubidium cell is shown, in its holder. The hairdryers can also be seen to the right in the picture.

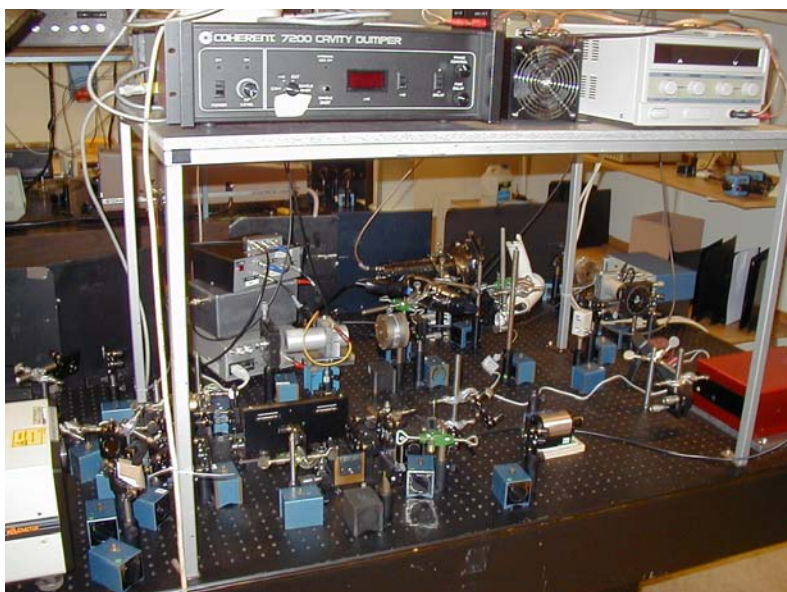


Figure 5-13: The experimental set-up in the laboratory. The red box to the right in the picture is the laser.

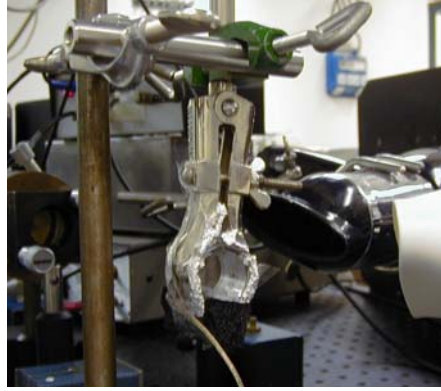


Figure 5-14: The Rubidium cell used in the experiments, in the middle of the picture. The hair-dryers used to heat the cell can be seen to the right in the picture.

Chapter 6

Further analysis of experiments

Initially there were several experimental steps in the plan of this master's thesis. However, only some of them, described in the previous chapter, were performed. Even if the other steps did not become a part of the experimental work carried out, some aspects of them were analysed. In this chapter some considerations of three-level echoes, with pulses coming from the same direction and with counterpropagating pulses, are discussed.

6.1 Long-lived three-pulse echo

In the previous chapter the effort to try to detect a two-pulse echo was described. The two-pulse echo only utilizes two levels. The long-lived three-pulse echo utilizes three levels, as in the scheme for the quantum state storage. For the echo to be long-lived, a storage state with a long lifetime is needed. The levels in Rubidium, to be used, are the same as the ones given for the quantum state storage in Chapter 3. To define the magnetic levels a magnetic field is to be applied over the cell. This will split the hyperfine levels into Zeeman components. A suggestion of an experimental set-up for long-lived three-pulse echo, with pulses from one direction, is illustrated in Figure 6-1.

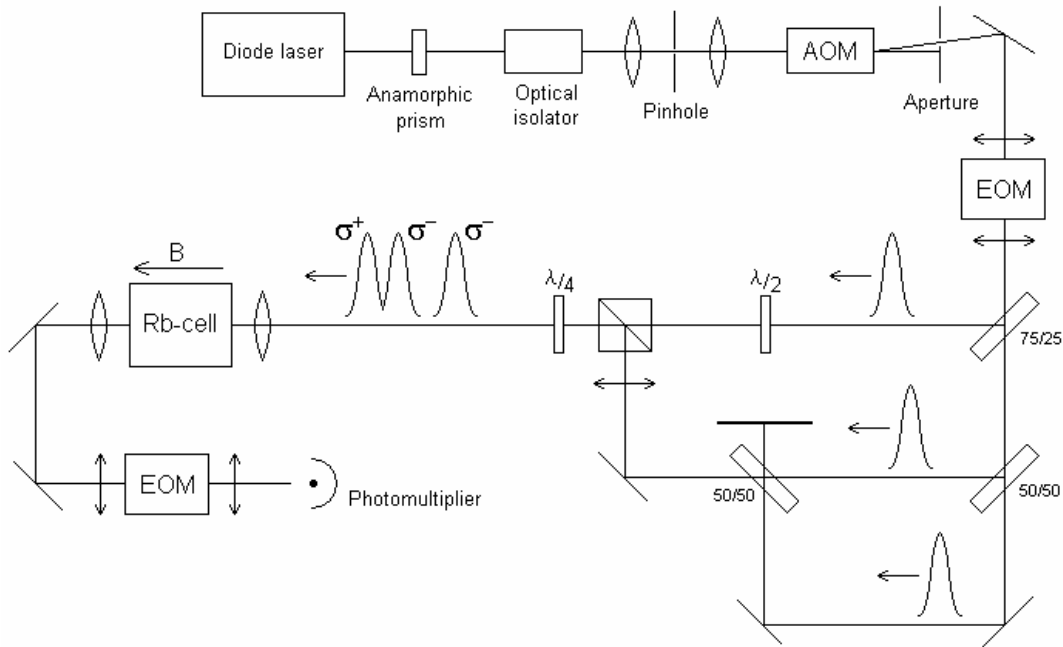


Figure 6-1: Experimental set-up for detection of a long-lived three-pulse photon echo. The excitation pulses and their polarisation are also shown in the picture. Beam splitters, which divide the intensity in 75/25 percent or 50/50 percent, are drawn in the picture. Further comments are given in the text.

The first and last parts are the same as for the two-pulse photon echo. However, now there is only one pulse generated by the AOM. It is divided into three pulses by beam splitters. The reason, that not all pulses can be generated from the AOM, is that they shall have different polarisations. The relative amplitudes of the different pulses can be chosen, by choosing the transmission / reflection ratio of the beam splitters. The first pulse passes a $\lambda/2$ -waveplate, which turns the linearly polarised light 90° .

When the beams are combined some light will be lost in the beam splitters. For the last combination a polarised beam splitter is used. Operated in the other direction it divides unpolarised light into two orthogonal linear polarised components. Used as it is here, the losses will be small since the beams to be combined have polarisations orthogonal to one another. The $\lambda/4$ -waveplate makes linear polarised light circularly polarised. It will be right-hand or left-hand polarised depending on the rotation of the plate compared to the direction of the polarisation before the plate. The direction of the magnetic field, compared to the propagation direction of the pulses, will then decide if the light will be σ^- or σ^+ polarised. The polarisation that the pulses should have after the $\lambda/4$ -waveplate are shown in the figure. Varying the optical path length for the different pulses changes the time separation between the pulses. A time separation of 22 ns between the first two pulses, as was the separation in the two-pulse echo experiment, corresponds to a difference in path length of around 7 meters.

The magnetic field across the cell shall be in the direction of propagation of the pulses, to achieve the correct polarisations for the scheme. The field should be weak, not to split the Zeeman levels too much. The separation between the levels should not be larger, than that the bandwidth of the laser pulse should cover both transitions. The field also needs to be homogenous throughout the sample, for the direction of it to be well defined. A Helmholtz coil pair, with the coils placed one on each side of the cell, best achieves this condition. To compensate for the vertical component of the earth magnetic field, another Helmholtz coil pair can be used. Placed above one another, one each side of the cell, the coils will generate a field in the opposite direction of the earth magnetic field. The total field component in the vertical direction inside the cell will then be cancelled.

To achieve the long-lived three-pulse echo, one pulse is divided into three pulses, as described above. The pulses will therefore be weaker than the pulses in the two-pulse echo. It will lead to a weaker echo, and the signal will therefore be even harder to detect than the two-pulse echo. Some improvements of the experimental set-up have to be done to be able to detect such an echo. Either the pulse power has to be increased, or the noise in the detection system has to be decreased further.

6.2 Three-level echo with counterpropagating pulses

The three-pulse echo described in this section is quite similar to the long-lived three-pulse echo described above. The three levels involved are the same, and therefore also the polarisation of the three pulses. In the echo considered here, the last pulse comes from a direction opposite to that of the first two pulses. This situation is analogous to that of the quantum state storage scheme. For the scheme to work with a high efficiency, the storage state must be emptied before the pulses are sent in. This can be achieved using optical pumping. An additional laser is to be used, together with the existing laser, for this purpose. Echoes generated in this way can be called high efficiency echoes, since the efficiency should be high, as in the quantum state storage process.

A suggestion of an experimental set-up for high efficiency photon echoes is illustrated in Figure 6-2. The zero order beam from the first AOM, which was blocked in the previous experiments, is now used for the optical pumping. It is combined with the beam from the second laser. A second AOM is used to turn on and off the pumping. In the other direction the second AOM lets the signal, which is going to be detected, through in the zero order beam. The first two pulses come from the same direction as in the previous arrangement. The third pulse, however, enters from the opposite direction, as shown in the figure. The echo will come out of the cell in the same direction as the third pulse. Since it is σ^+ polarised and travels in the opposite direction than the two first pulses, it will follow the path of the second pulse. It will therefore be separated from the third pulse, which will follow the path of the first pulse. The signal will be led off to the detector by one of the beam splitters. The disadvantage with this separation of the signal is that half the signal intensity will be lost in the beam splitter.

Another way of aligning the beams are by letting them enter by a small difference in angle. The echo will then be separated by a small angle from the other beams. A set-up like this will simplify the alignment and the detection. The intensity of the echo will however decrease with the angle of

separation. The interacting volume will be smaller. There will also be a small error due to the fact that the direction of the Doppler shift will not be exactly the opposite for the two beams.

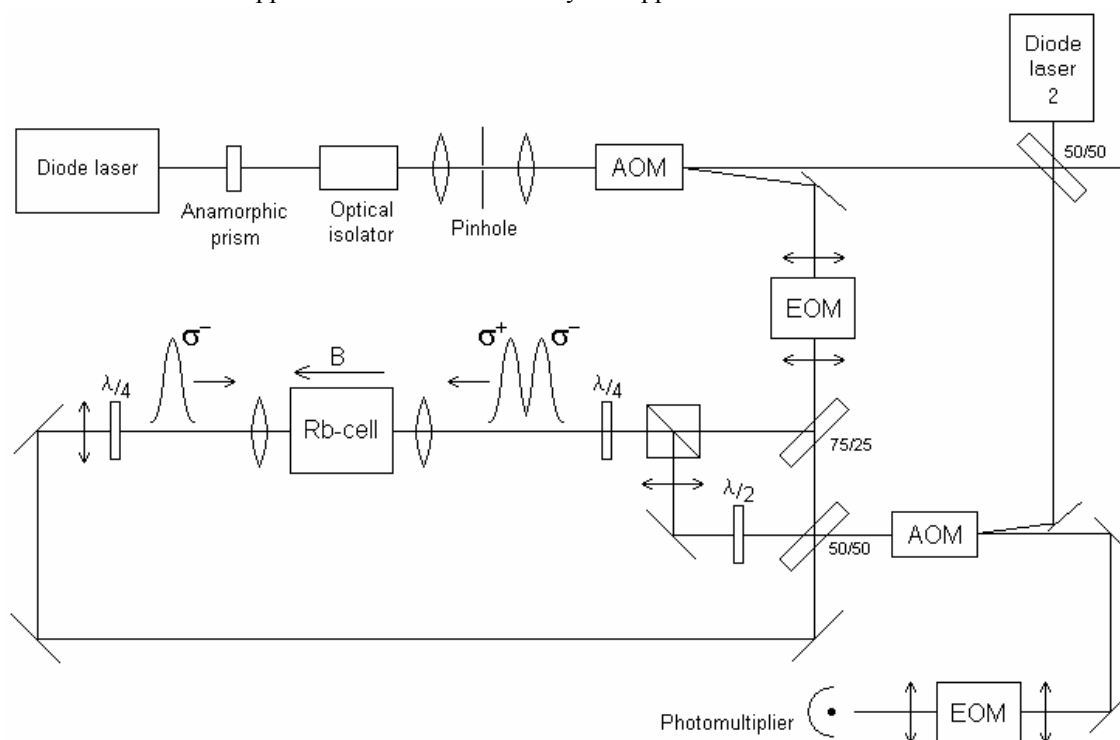


Figure 6-2: Experimental set-up for three-level echo with counterpropagating pulses. The three excitation-pulses are illustrated in the picture. The components for the pumping are also shown. Further comments on the picture are given in the text.

To find out if the optical pumping of the atoms is good the fluorescence from the cell can be studied. When it disappears the number of atoms in the quantum state storage ground state is high. Only the atoms that are not pumped will then be excited, and therefore the number of fluorescing atoms will decrease. The pumping shall be turned off just shortly before the pulses enter the cell. As the time increases the atoms will relax back to the storage state. This will make the echo much harder to detect.

To carry out quantum state storage, of single-photon wave packets, experimentally is a lot more complicated. The first step then would be to generate the single-photon wave packet and combine its path with the second pulse. The second and third pulse has to be very close to π -pulses, for the process to be reliable. The experiment would probably have to be performed in vacuum, where no other atoms are present to interact with the single photon. Then the problem arises, how the Rubidium atoms should be isolated. If a cell is used there is a probability that the single photon will be reflected in the optical surface of the cell. Another aspect is that, when the photon is recalled it will be hard to subtract it from the noise in the signal. Since the readout photon will come within a well-defined solid angle, the noise can be reduced by detecting the signal within a narrow angle. Noise from spontaneous emission, for example, will be emitted in all directions. It will therefore be suppressed quite effectively as the angle of detection is decreased.

Chapter 7

Conclusions

The work of this master's thesis has been a step on the way to experimentally carry out the quantum state storage scheme introduced in reference [4]. There have to be additional thoughts put into high-efficiency photon echoes, before the experimental work can be continued. No photon echoes were detected during the work of this thesis. There might be one or many reasons for that. It is not yet known why an echo could not be detected. The calculations and assumptions made in this thesis must be studied further. Going through the experimental set-up again is also a step on the way to find out what can be improved. It must also be analysed whether the experimental equipment available, in the photon echo group, is sufficient.

A lot of knowledge was gained regarding experiments of the kind conducted in this master's thesis. No similar experimental work has been carried out previously in the photon echo group. Particularly working on such a short timescale has not been done before. Therefore problems that came across were not as simple to solve, as they would have been if similar problems were known to the group.

In the experimental work done, it was found that the pulses were harder to generate than expected. The pulse finally generated might be good enough, although it was not as good as desired. If the pulses were shorter an echo would be easier to detect. The pulses would then easily be separated, leading to less background when the echo appears. The pulse separation could also be made shorter, if the pulse duration was shorter, which would increase the intensity of the echo. With the equipment available at the time I think it will be hard to generate pulses of much shorter duration.

Other materials can be investigated as alternatives to Rubidium. One material to examine further is Ytterbium, where longer pulses could be used, and there might be others that could be a good idea to analyse. Finally it can be said that, although the work in this master's thesis has given a considerable better understanding of how the experiments should be carried out, there is still a long way to go to demonstrate the quantum state storage scheme.

Acknowledgements

I want to give a special thank you to my supervisor Prof. Stefan Kröll, for giving me the opportunity to have this interesting and instructive project as my diploma work. I also want to thank him for his help and engagement along the way.

Further I would like to thank Lars Rippe, Mattias Nilsson and Andreas Walther for the valuable discussions, for all the questions they answered and for the help in the lab.

I also want to thank Åke Bergquist for all help with the electrical equipment, and Anders Persson for borrowed equipment.

A warm thank you to my family and Daniel for their support.

Finally I want to thank all that I have not mentioned above, for the help you have given me.

Bibliography

- [1] Pinkse PW, Fischer T, Maunz P, Rempe G., *Trapping an atom with single photons*, Nature, Vol. 404, p. 365-368 (2000)
- [2] D. F. Phillips, A. Fleischhauer, A. Mair, R.L. Walsworth and M. D. Lukin, *Storage of Light in Atomic Vapor*, Physical Review Letter, Vol. 86, No 5 (2001)
- [3] M. Fleischhauer, S.F. Yelin, M.D. Lukin, *How to trap photons? Storing single-photon quantum states in collective atomic excitations*, Opt. Commun., Vol. 179, 395 (2000)
- [4] S. A Moiseev, S. Kröll, *Complete Reconstruction of the Quantum State of a Single-Photon Wave Packet Absorbed by a Doppler-Broadened Transition*, Physical Review Letter, Vol. 87, No 17 (2001)
- [5] S.A. Moiseev, V.F. Tarasov, B.S. Ham, *Quantum memory photon echo-like techniques in solids*, J. Opt. B: Quantum Semiclass. Opt. 5 (2003)
- [6] M. Nilsson, S. Kröll, *Solid state quantum memory using tailored and externally controlled inhomogeneous absorption profiles and photon-echo-like techniques*, accepted for publication in Opt. Comm. (2004)
- [7] S. Kröll, *Coherent transient spectroscopy*, laboratory instructions in the course Atomic and Molecular Spectroscopy, Lund Institute of Technology
- [8] A V Durrant, J Manners, P M Clark, *Understanding optical echoes using Schrödinger's equation: I. Echoes excited by two optical pulses*, Eur. J. Phys. 10, p. 291-297, (1989)
- [9] M. Nilsson, *Coherent Interactions in Rare-Earth-Ion-Doped Crystals for applications in Quantum Information Science*, Doctoral Thesis, LRAP-333.
- [10] Daniel A. Steck, *Rubidium 87 D Line Data*, Theoretical Division, Los Alamos National Laboratory, <http://george.ph.utexas.edu/~dsteck/alkalidata/rubidium87numbers.pdf>, (2001)
- [11] Robert C. Hilborn, *Einstein coefficients, cross section, f values, dipole moments, and all that*, Am. J. Phys. 50(11), (1982)
- [12] Lars Levin, *Construction and design of an electro-optically tuneable mode-hop free external cavity diode laser*, Lund Report on Atomic Physics, (2000)
- [13] Frank L. Pedrotti, S.J., Leno S. Pedrotti, *Introduction to optics*, Second Edition, Prentice-Hall International
- [14] *Do you know Acousto-optics? Application notes*, A-A Opto-Electronic, <http://www.a-a.fr/General/Acousto-optic-Info.html>
- [15] Sven-Göran Pettersson, Stig Borgström, Hans Hertz, *Optisk teknik*, Dept. of Physics, LTH, (1996)
- [16] Orazio Svelto, *Principles of Lasers*, Plenum Press, fourth edition, (1998)
- [17] Yong-qing Li, Min Xiao, *Electromagnetic induced transparency in three-level A-type system in rubidium atoms*, Physical Review A, Vol. 51, No 4 (1995)
- [18] S. Kröll and p. Tidlund, *Recording density limit of photon-echo optical storage with high-speed writing and reading*, Applied Optics, Vol. 32, No 35 (1993)

Appendix A

Quantum state storage calculations for Rubidium

A.1 Pulse areas

To clarify the requirements for doing quantum state storage in Rubidium, some calculations are needed. From the expression of the oscillator strength in the section above the electric dipole moment is found. For the whole D1 transition, which is the one used in the two-pulse photon echo to be conducted, $f = 0.3420$ and the dipole moment is [11]

$$|\mu| = \sqrt{\frac{3\hbar e^2}{2m\omega}} \cdot f = 2.537 \cdot 10^{-29} \text{ Cm}$$

To achieve a π -pulse, a certain amplitude of the electric field is needed. It could be found from the expression of the pulse area in chapter 2. A pulse length of $T = 10$ ns is assumed.

$$E_0 = \frac{\hbar\theta}{2\mu T} = 653 \text{ V/m}$$

The intensity of the light is given by

$$I = 2n \sqrt{\frac{\epsilon_0}{\mu_0}} |E|^2 \propto \frac{1}{f}$$

where n is the refractive index, and ϵ_0 is the capacitivity for free space. μ_0 is the permeability for free space. The intensity turns out to be proportional to one over the oscillator strength. If the approximation that for the Rubidium gas $n = 1$ is done, the intensity required is 2.26 kW/m^2 . For the quantum state storage higher intensities are required, since not the whole D1 transition is used. For the transition $m = -2$ to $m = -1$, the oscillator strength is $0.3420 / 6$. The intensity, to achieve a π -pulse, is found to be six times the intensity for the whole transition, $I = 13.6 \text{ kW/m}^2$. For the $m = -1$ to $m = 0$ transition $f = 0.3420 / 4$, corresponding to an intensity of 9.05 kW/m^2 , to achieve a pulse area of π .

To get such high intensities the beam has to be focused. Lets assume that the peak power of the light pulse is 0.5 mW before the cell. The highest intensity needed, in the quantum state storage process, then corresponds to an area of $3.7 \cdot 10^{-8} \text{ m}^2$. The beam does not have a uniform intensity distribution throughout its cross section. For a Gaussian intensity distribution, the area of the beam can be defined by the point where the intensity has gone down by a factor $1/e^2$ of the intensity in the middle of the beam. The radius of the beam, defined in the same way as the area above, is called the beam spot size. The beam spot size at a distance z from focus is given by [A.1]

$$w^2(z) = w_0^2 \left(1 + \left(\frac{z\lambda}{\pi w_0^2} \right)^2 \right)$$

where w_0 is the spot size at focus. If the beam is parallel before the lens the distance z corresponds to the focal length of the lens. The area calculated above corresponds to a radius of $108 \mu\text{m}$. The radius of the beam is assumed to be $w = 0.5 \text{ mm}$ before focusing. If the beam is approximated to be Gaussian, the focal spot should then be $z = 0.21 \text{ m}$ away, to achieve a radius of $108 \mu\text{m}$ in focus. This means that a lens with focal length 20 cm is a good choice. The beam radius at the ends of the cell, which is 2.5 cm long, is found by setting $z = 1.25 \text{ cm}$. It is calculated to be $112 \mu\text{m}$. This variation of the beam size throughout the cell corresponds to a variation of the pulse area of 3.6% . Such a variation could be considered as acceptable.

For the two-pulse echo to be carried out, the beam does not have to be focused that hard. A beam spot size of 265 μm is needed in this case. If the beam again is assumed to have a beam spot size of 0.5 mm before focusing, any lens with a focal length of less than 44 cm can be used.

A.2 Vapour pressure

The transmission of light through a sample of atoms is given by

$$I = I_0 \cdot e^{-\alpha L}$$

where I_0 is the intensity before the sample and L is the length of the sample. α is the absorption coefficient and it depends on the frequency of the light. The cross section for absorption, σ , is related to the absorption coefficient as [11]

$$\alpha = \frac{N}{V} \cdot \sigma$$

where N/V is the number of atoms per volume unit, contributing to the absorption. From the oscillator strength the cross section is found by [11]

$$\sigma = \frac{\pi e^2}{2\epsilon_0 mc} f \cdot g(\omega)$$

where $g(\omega)$ is line shape function for the broadening of the transition. For Doppler broadening the line shape function is [16]

$$g(\omega) = \frac{1}{\omega_0} \sqrt{\frac{2\pi Mc^2}{kT}} e^{-\frac{Mc^2}{2kT} \left(\frac{\omega - \omega_0}{\omega_0}\right)^2}$$

where T is the temperature in Kelvin and k is Boltzmanns constant. M is the mass of an atom, for ^{87}Rb $M = 87\text{u} = 1.44 \cdot 10^{-25}$ kg. At the centre frequency of the transition the line shape function has the value

$$g(\omega_0) = \frac{1}{\omega_0} \sqrt{\frac{2\pi Mc^2}{kT}}$$

This is the expression used since the laser frequency is set to the transition frequency in the quantum state storage process. If all these expressions are united it could be seen that the absorption in a sample depends on both the concentration of atoms and the temperature, as follows

$$\alpha = \frac{N}{V} \cdot \frac{\pi e^2}{2\epsilon_0 mc} f \cdot \frac{1}{\omega_0} \sqrt{\frac{2\pi Mc^2}{kT}}$$

There is also another formula that relates the concentration to the temperature in any gas. The ideal gas law is given by

$$pV = NkT$$

where N is the total number of atoms, and p is the pressure. In the quantum storage experiment that will be carried out, it is only the ^{87}Rb atoms that are contributing to the absorption. Since the natural composition of Rubidium contains 27 % ^{87}Rb , the relation between the number of ^{87}Rb atoms and the total number of rubidium atoms is

$$N_{87} = 0.27 \cdot N$$

Again uniting the expressions, the absorption can be given as a function of pressure and temperature.

$$\alpha = 0.27 \frac{p}{kT} \cdot \frac{\pi e^2}{2\epsilon_0 mc} f \cdot \frac{1}{\omega_0} \sqrt{\frac{2\pi Mc^2}{kT}} = \text{const} \cdot \frac{p}{T^{3/2}} \cdot f$$

For a given temperature, the pressure in a gas will always be set by the vapour pressure. If there is an amount of solid Rubidium, more and more of it will vaporize as the temperature is increased. The vapour pressure as a function of temperature is given in a curve in [10]. To find a wanted absorption, iterations between the formula above and the vapour pressure curve are done.

To achieve the highest photon echo intensity, in a normal two-pulse echo, it has been shown that an absorption of $\alpha L \approx 1$ is desirable. This corresponds to a transmission through the cell of 37 %. L is the length of the sample, which in our case is 2.5 cm. The absorption coefficient α should then be around 40 m^{-1} . For a two-pulse echo, which is to be carried out, the oscillator strength is again 0.342. From the above formula, and the vapour pressure, the temperature is calculated to be 28°C to achieve the desired absorption. At this temperature the concentration of ^{87}Rb atoms is $3.8 \cdot 10^{15} \text{ m}^{-3}$.

If a three level echo is to be carried out by beams in the same direction, $\alpha L \approx 1$ is still desirable. Consider such an echo where the levels is the same as for the quantum state storage. The smallest oscillator strength for the transitions involved is then 0.0570. The temperature required in this case is calculated to be 48°C , in the same way as above. For the quantum state storage experiment, with counter propagating pulses, it is instead desirable to have a high absorption, $\alpha L \gg 1$. For $\alpha L = 10$, the absorption coefficient will be $\alpha = 400 \text{ m}^{-1}$. Then the transmission will be 0.0045 %, which should be good enough. The smallest oscillator strength is still 0.0570, leading to a temperature of 77°C . The concentration of ^{87}Rb atoms at this temperature is $2.4 \cdot 10^{17} \text{ m}^{-3}$.

The calculations above are valid if there are much more atoms in the sample than photons in the pulse. If the number of photons is of the same order as the number of atoms, the absorption will be affected. Then the last photons in the pulse will experience fewer atoms in the sample, because some have already been excited. The volume of the beam inside the cell is

$$V = \pi r^2 L = 9.2 \cdot 10^{-10} \text{ m}^3$$

where $r = 108 \text{ }\mu\text{m}$, and $L = 2.5 \text{ cm}$ is used. From the concentrations above, the number of atoms in the beam path at 28°C is $N_{atoms} = 3.4 \cdot 10^6$, and at 77°C it is $N_{atoms} = 2.2 \cdot 10^8$. The pulse is again assumed to have a power of 0.5 mW before the cell and a duration of $t = 10 \text{ ns}$. Then the number of photons in a pulse is given by

$$N_{photons} = \frac{P \cdot t}{\hbar \omega} = 2.0 \cdot 10^7$$

It can be seen that the number of photons is greater than the number of atoms at 28°C . At 77°C there are only ten times more atoms than photon, which is not much. Therefore the results calculated above can't be used right of to get a desired absorption. To increase the absorption the temperature can be increased to a point were the desired absorption could be seen in the signal.

A.3 Requirements for quantum state storage

There are some requirements for the quantum state storage scheme stated in chapter 2. One of these is that the Doppler profile should be much larger than the spectral width of the pulse. The full width half maximum, FWHM, of the Doppler broadening line shape function is given by [16]

$$\Delta\omega_d = \frac{2\omega_0}{c} \sqrt{\frac{2kT \ln 2}{M}}$$

At the temperature calculated above for the quantum state storage, $T = 77^\circ\text{C}$, the Doppler broadening is 540 MHz. From the formula for the minimum pulse duration, in the beginning of chapter 5, the bandwidth of a transform-limited pulse can be calculated. For a pulse length of 10 ns, the bandwidth is 44 MHz. Since this is much smaller than the width of the Doppler broadening, the condition on the spectral width of the pulse is fulfilled.

Another condition to be fulfilled is that the coherence time should be long in comparison with the storage time. The coherence time depends on the homogenous broadening due to spontaneous decay and to collisions between atoms. For the excited state the lifetime due to spontaneous decay has already been discussed. For the storage state the collisions will probably be the dominating homogenous broadening mechanism. The time between the collisions can be estimated, by use of the hard sphere model, to be [16]

$$\tau_c = \sqrt{\frac{2}{3}} \cdot \frac{1}{8\pi} \frac{\sqrt{MkT}}{pa^2}$$

where p is the pressure and a is the radius of the atom, which is approximately 0.25 nm for a Rubidium atom. Here the average mass of all rubidium atoms should be used, $M = 85.5$ u, because both isotopes contribute to the collision broadening. At 77 °C the coherence time is found to be $\tau_c = 3.2$ ms. Since this time is rather long it will not be a problem to the storage process. The atoms moving out of the beam path would instead be a larger problem. The average velocity of the ^{87}Rb atoms, at 77 °C, is given by

$$v = \sqrt{\frac{8kT}{\pi M}} = 292\text{m/s}$$

The time it takes for the atoms to travel through a beam, with a diameter of 108 μm , is then 371 ns. This will be the factor setting the limit to how long the storage time can be.

Appendix B

Intensity of a two-pulse echo

The number of photons, S , in a two-pulse echo, where the pulses has the pulse area θ_1 and θ_2 respectively, can be calculated from the following formula taken from reference [18].

$$S = \left(\frac{N}{2V} A \cdot L \frac{T_{inh}}{\tau_{dur}} \right)^2 A_{21} \tau_{dur} \frac{3\lambda}{8Ln} e^{-2T/\tau} \sin^2 \theta_1 \left(\sin^2 \frac{\theta_2}{2} \right)^2$$

The first part, within brackets, describes how many atoms are in the beam path, and in the right frequency interval. Here N/V is the concentration of atoms, A is the area of the beams cross-section and L is the length of the sample. T_{inh} is the inhomogeneous relaxation time, related to the inhomogeneous linewidth as $\Delta\nu = 1/(\pi T_{inh})$, and τ_{dur} is the duration of the excitation pulses. The pulses must be Fourier limited for the formula to be valid. The exponential term arises from the spontaneous decay during the time separation, T , between the first pulse and the echo. τ is the lifetime of the excited state. Other homogeneous broadening mechanism, such as collisions, are neglected. A_{21} is the Einstein coefficient for spontaneous decay for the transition, and it is equal to $1/\tau$. For the D1 transition A_{21} is found to be $3.61 \cdot 10^9 \text{ s}^{-1}$. n is the refractive index, again approximated to be equal to one. T_{inh} is found, from the calculated value of The Doppler linewidth in Appendix A, to be 0.59 ns.

To get a desired absorption when looking for the two-pulse echo, the cell was heated to approximately 59 °C. From the vapour pressure formulas in Appendix A, the concentration of ^{87}Rb atoms at this temperature is found to be $N/V = 2.6 \cdot 10^{16} \text{ m}^{-3}$. The length of the cell is $L = 2.5 \text{ cm}$, and the pulse duration was around 10 ns. With a lens of focal length 15 cm, and a beam spot size of 0.5 mm before focusing, the focus spot size becomes 77 μm . Here the formula of the beam spot size in Appendix A has been used, rewritten as

$$w_0^2 = \frac{w^2}{2} - \sqrt{\frac{w^4}{4} - \frac{z^2 \lambda^2}{\pi^2}}$$

The beam size at the ends of the cell, $z = 1.25 \text{ cm}$, is then 87 μm . To calculate how large the area of the beam is inside the cell an average of the radius is used, $(77 + 87) / 2 = 82 \mu\text{m}$. The peak power of the two pulses was around 450 μW before entering the cell. Using the formulas from Appendix A the pulse areas are calculated to be $\theta_1 = \theta_2 = 3.1\pi$. The time separation between the first pulse and the echo was $T = 44 \text{ ns}$. The number of photons in the echo is found to be $2.8 \cdot 10^5$. This could be compared to the number of photons in a pulse, $2.0 \cdot 10^7$, calculated in appendix A. The expected echo should have an intensity of 1.4 percent of the excitation pulses. However, in these calculations the absorption of the echo on the way out of the sample is not considered. When this is also taken into account, the echo will have less intensity than calculated above.

With both the excitation pulses equal in strength, the optimum number of photons is found with a pulse area of $\theta_1 = \theta_2 = 2\pi/3$. With all the other settings, in the experiment, unchanged there would be $1.3 \cdot 10^6$ photons in the echo. This is almost five times as many as for the pulse areas above.